Exploring non-standard $Hb\bar{b}$ interactions at future electron-proton colliders

arXiv:2305.05462

IPM Wednesday Weekly Seminar

Presented by:
Reza Jafari*

In Collaboration with:
H. Khanpour, M. Mohammad, H. Haghighat

School of Particles and Accelerators, IPM

24 May 2023

* jafari@ipm.ir

OUTLINE

- Introduction
- Theoretical framework
- Data Simulation
- Analysis strategy
- Results & discussion
- Conclusion

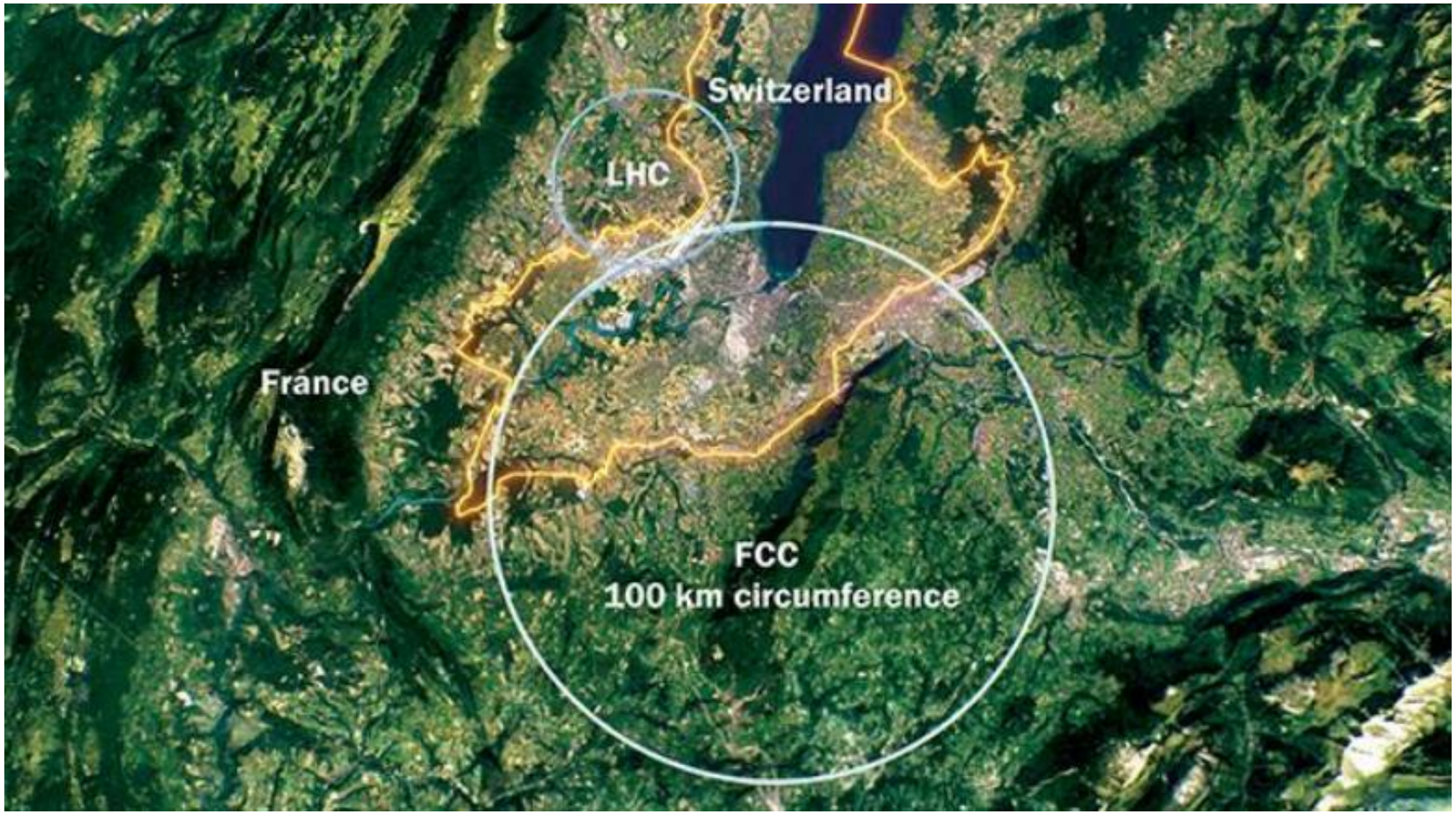

INTRODUCTION

- After the Higgs boson discovery, the focus shifted toward understanding its couplings to other particles, in particular to the fermions.
- Exploring CP nature of the Higgs couplings has become very important.

CP violation in the Higgs sector → impact on Baryogensis problem

The Yukawa coupling of H to the 3rd generation fermions is larger.

Therefore, studying of CP properties with them play an important role.

INTRODUCTION

A crucial aspect ⇨ Measurement of the b-quark Yukawa coupling

- To check the consistency of the SM and BSM.
- Extensive studies have been performed over the years to assess the feasibility of this measurement.
- Nevertheless, the observation of the H → bb decay remains very challenging at the LHC.

Recently, there has been a consideration for high energy ep collisions at the LHC.

A rich physics program | **Very exciting prospects** | **Direct extraction of y_b**

INTRODUCTION

- **Tentative schedule for the LHeC project.**

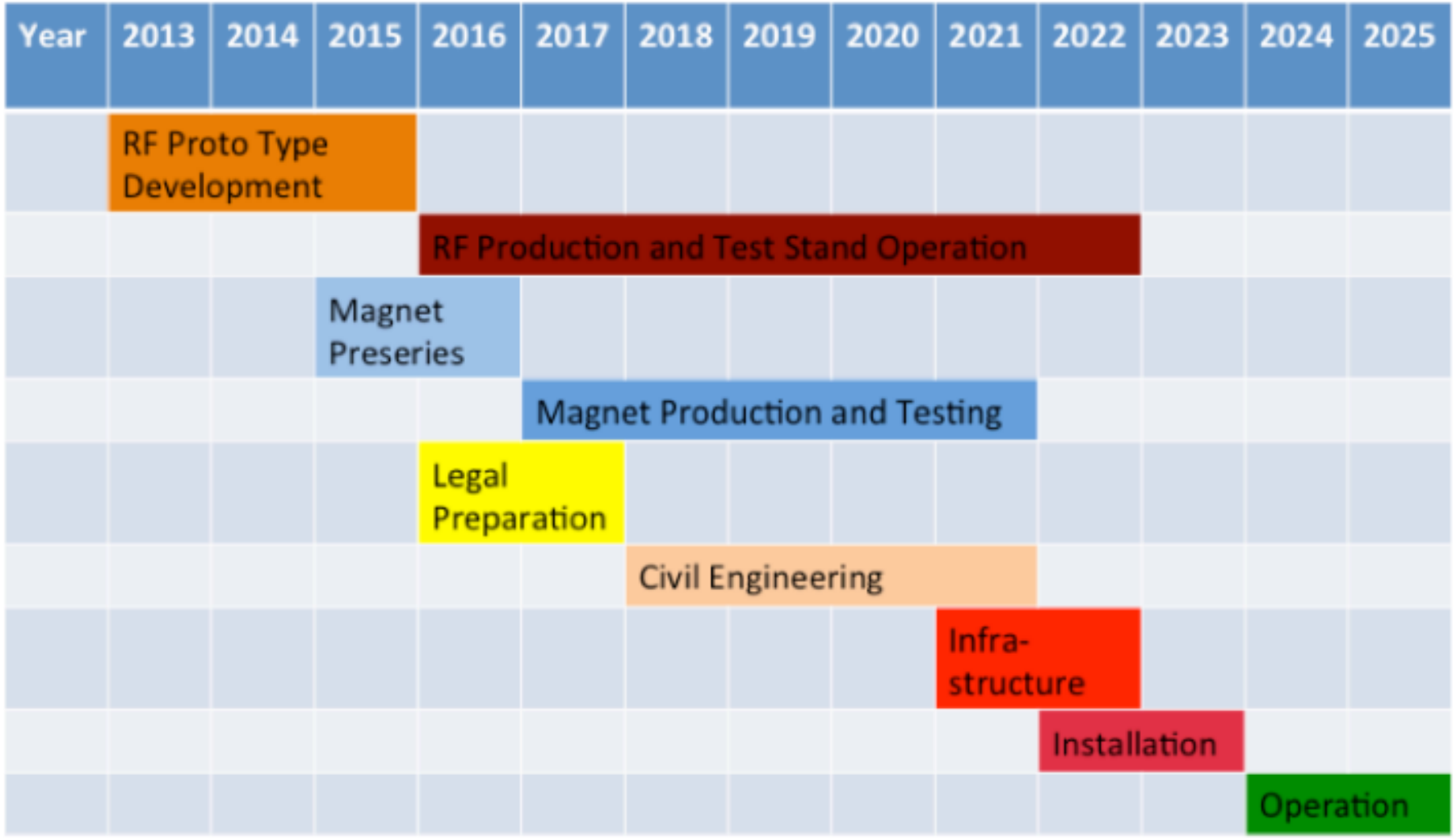

INTRODUCTION

- **Other ep colliders more than LHeC at CERN:**

FCC-ee | FCC-hh | FCC-eh ★

- **Benchmarks:** $E_e = 60\,\mathrm{GeV}$

	Unit	LHeC	HE-LHeC	FCC-eh	FCC-eh
E_p	TeV	7	13.5	20	50
$\sqrt{s}$	TeV	1.30	1.77	2.2	3.46

$$\sqrt{s} = 2\sqrt{E_p E_e}$$

INTRODUCTION

- **Other ep colliders more than LHeC at CERN:**

FCC-ee | FCC-hh | FCC-eh ★

- **Benchmarks:** $E_e = 60\,\mathrm{GeV}$

	Unit	LHeC	HE-LHeC	FCC-eh	FCC-eh
E_p	TeV	7	13.5	20	50
$\sqrt{s}$	TeV	1.30	1.77	2.2	3.46

$$\sqrt{s} = 2\sqrt{E_p E_e}$$

INTRODUCTION

- **Higgs Production at ep collision:**
- **Leading order SM diagrams for *Neutral Current (NC)*:**

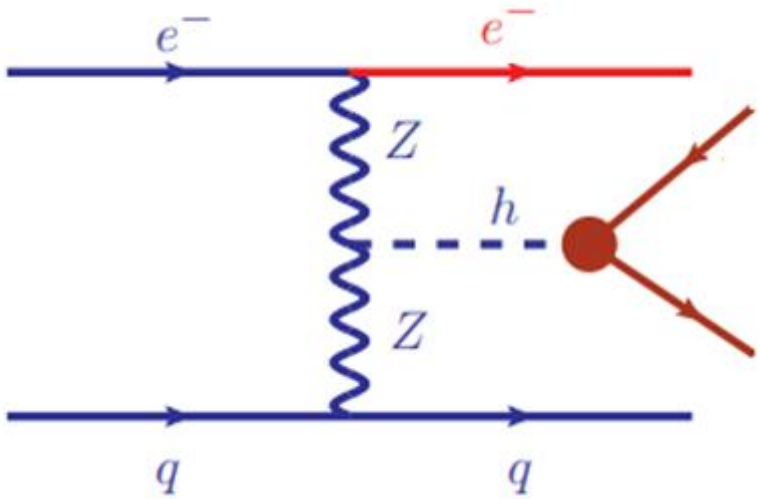

$$eq \to eHq$$

VBF process

INTRODUCTION

- **Higgs Production at ep collision:**
- **Leading order SM diagrams for *Charged Current (CC)*:**

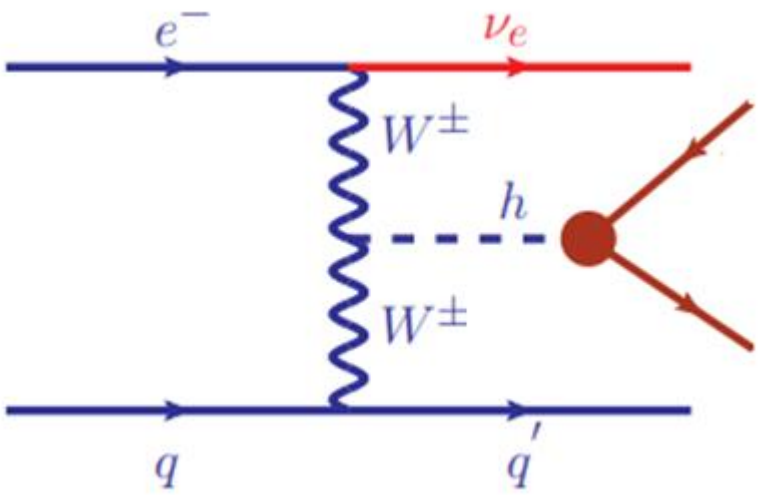

$$eq \to \nu_e H q'$$

VBF process

INTRODUCTION

- **Higgs Production at ep collision:**
- Leading order SM diagrams for CC (NC) processes:

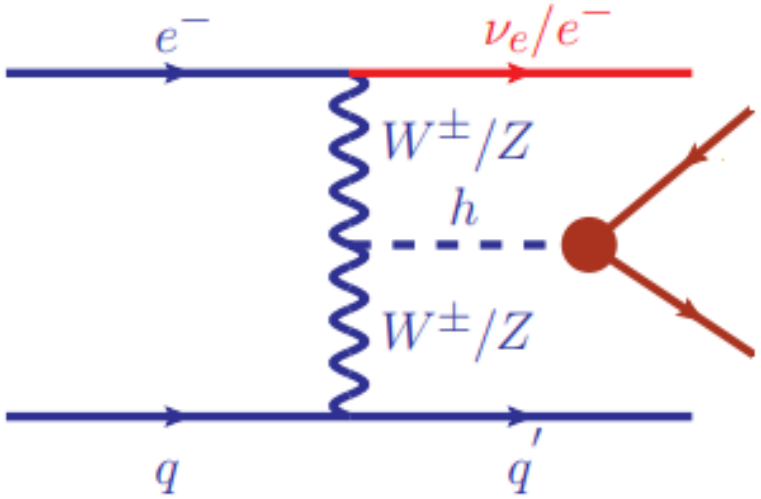

- **VBF processes:**

$$eq \to \nu_e H q' \quad \text{and} \quad eq \to eHq$$

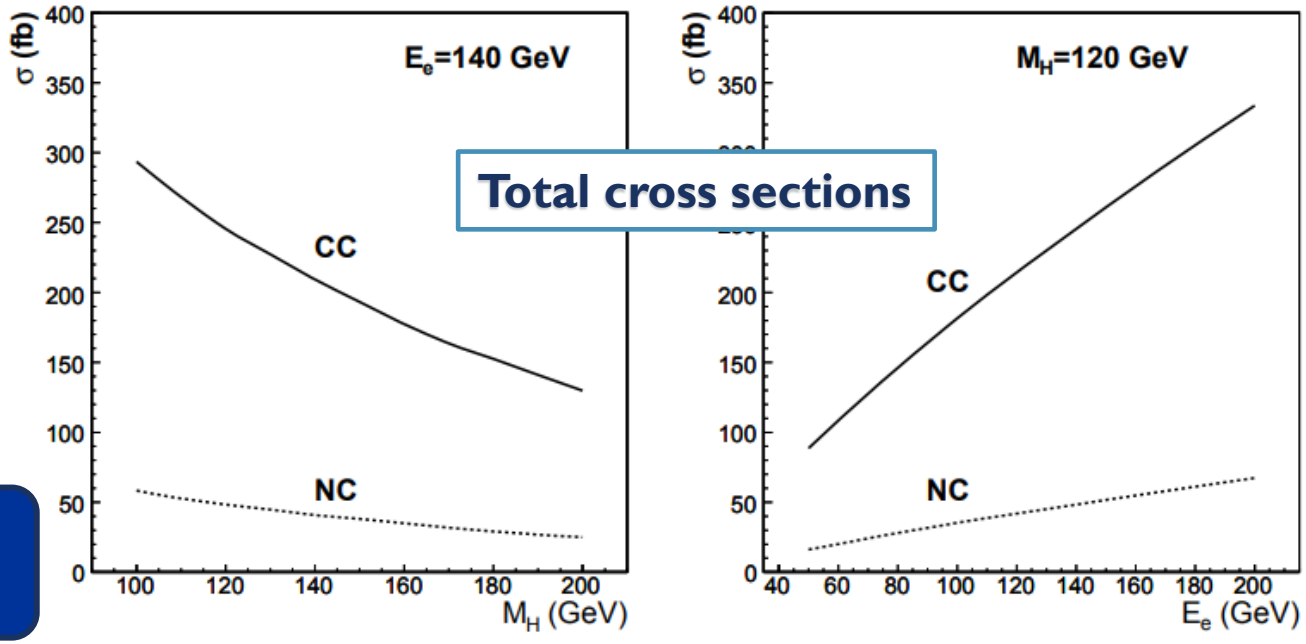

Total cross sections

the production rate of CC is larger than NC process by about a factor of 4 − 6

THEORETICAL FRAMEWORK

- ***Standard Model Effective Field Theory (SMEFT)***

$$\mathcal{L}_{\text{SMEFT}} = \mathcal{L}_{\text{SM}} + \sum_i \frac{c_i \mathcal{O}_i}{\Lambda^2}$$

- **A proper formalism of the impacts of new physics is to consider SM as an effective theory.**
- **SMEFT is a powerful tool to examine deviations from the SM.**
- **Non-standard couplings can be parameterized by operators of d > 4. The leading effects for collider observables typically enter at d=6.**

THEORETICAL FRAMEWORK

- **The effective Lagrangian for mass and Yukawa terms:** [arXiv:9909265]

$$\mathcal{L}_f = \frac{y_f v}{\sqrt{2}}\left[1+\frac{v^2}{2\Lambda^2}\frac{X_R^f+iX_I^f}{y_f}\right]\overline{f_L}f_R + \frac{y_f}{\sqrt{2}}\left[1+\frac{3v^2}{2\Lambda^2}\frac{X_R^f+iX_I^f}{y_f}\right]\overline{f_L}f_R h + \frac{3v}{2\sqrt{2}\Lambda^2}\left(X_R^f+iX_I^f\right)\overline{f_L}f_R hh + \frac{1}{2\sqrt{2}\Lambda^2}\left(X_R^f+iX_I^f\right)\overline{f_L}f_R hhh$$

- Λ : the energy scale of new physics
- y_f : Yukawa coupling for the relevant fermion
- $X_{R,I}$: Real and Imaginary part of coefficients of the dimension-six terms.

$$X_i^b \equiv \frac{2\Lambda^2}{v^2} y_b T_i^b,$$

DATA SIMULATION

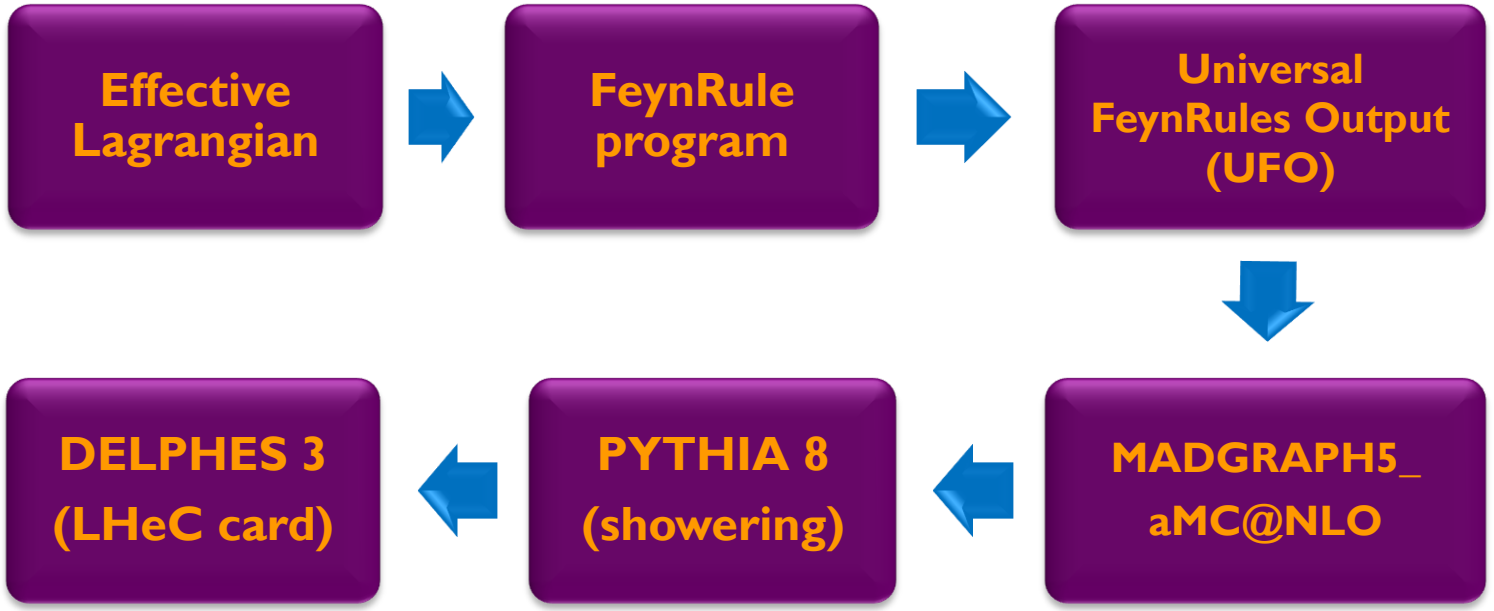

- Two different signal samples ≡ Two T_I and T_R coefficients
- Dimension-six operator coefficients $T_{I,R}$, with Λ = 1 TeV.

DATA SIMULATION

- **Signals and SM background cross section as a function of E_e (left) and E_p (right).**

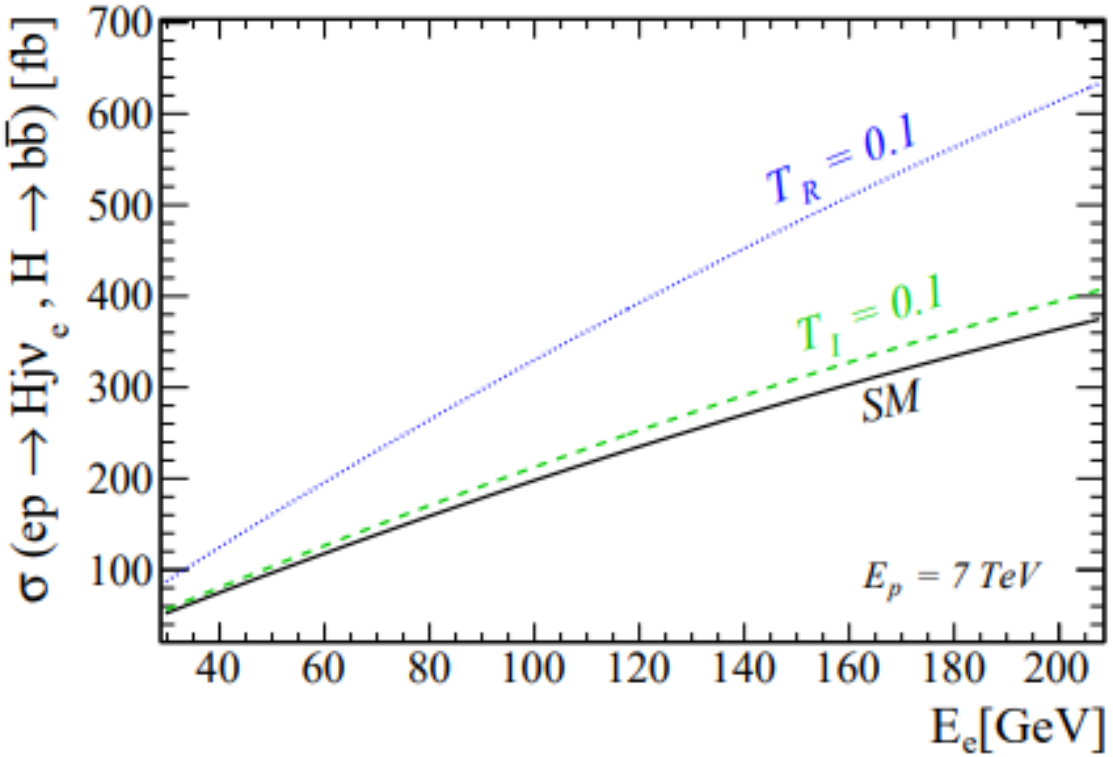

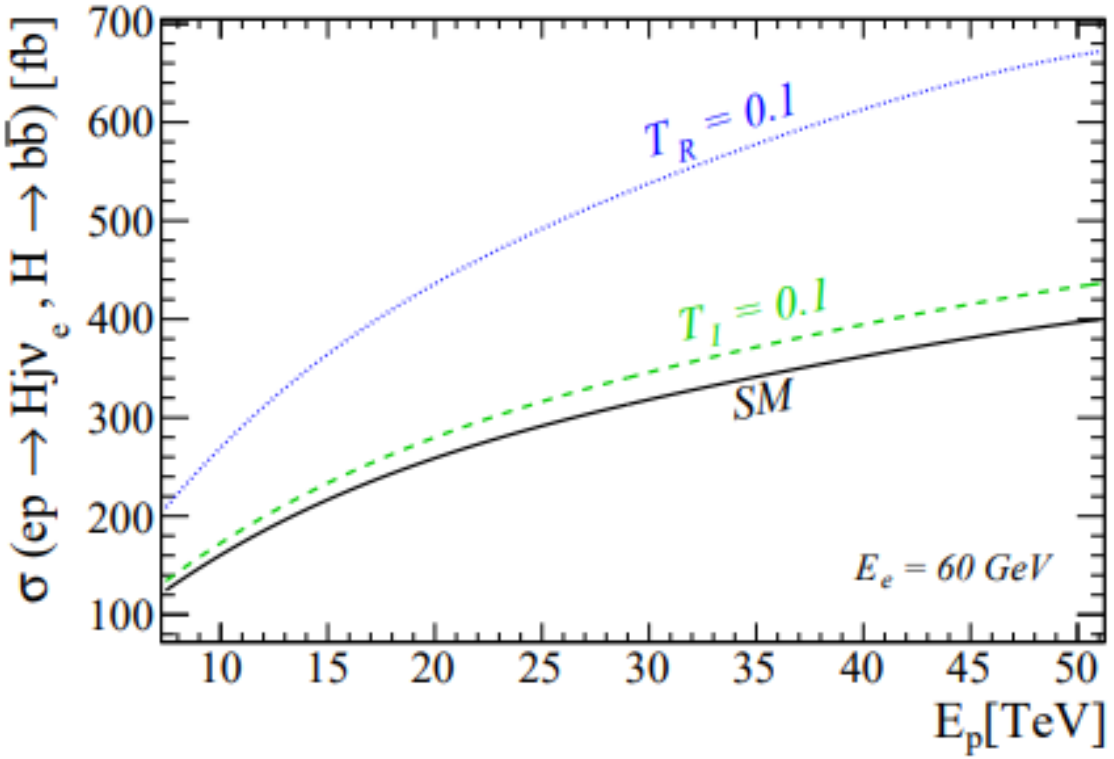

DATA SIMULATION

$$\sigma(e^- p \to H j \nu_e,\ H \to b\bar{b})(T_i) = \sigma_{\mathrm{SM}} + \alpha_i T_i + \beta_i T_i^2,$$

- Signal cross section as a function of T_I and T_R coefficients
- For $T_R = -1/3$ cross section goes to zero.

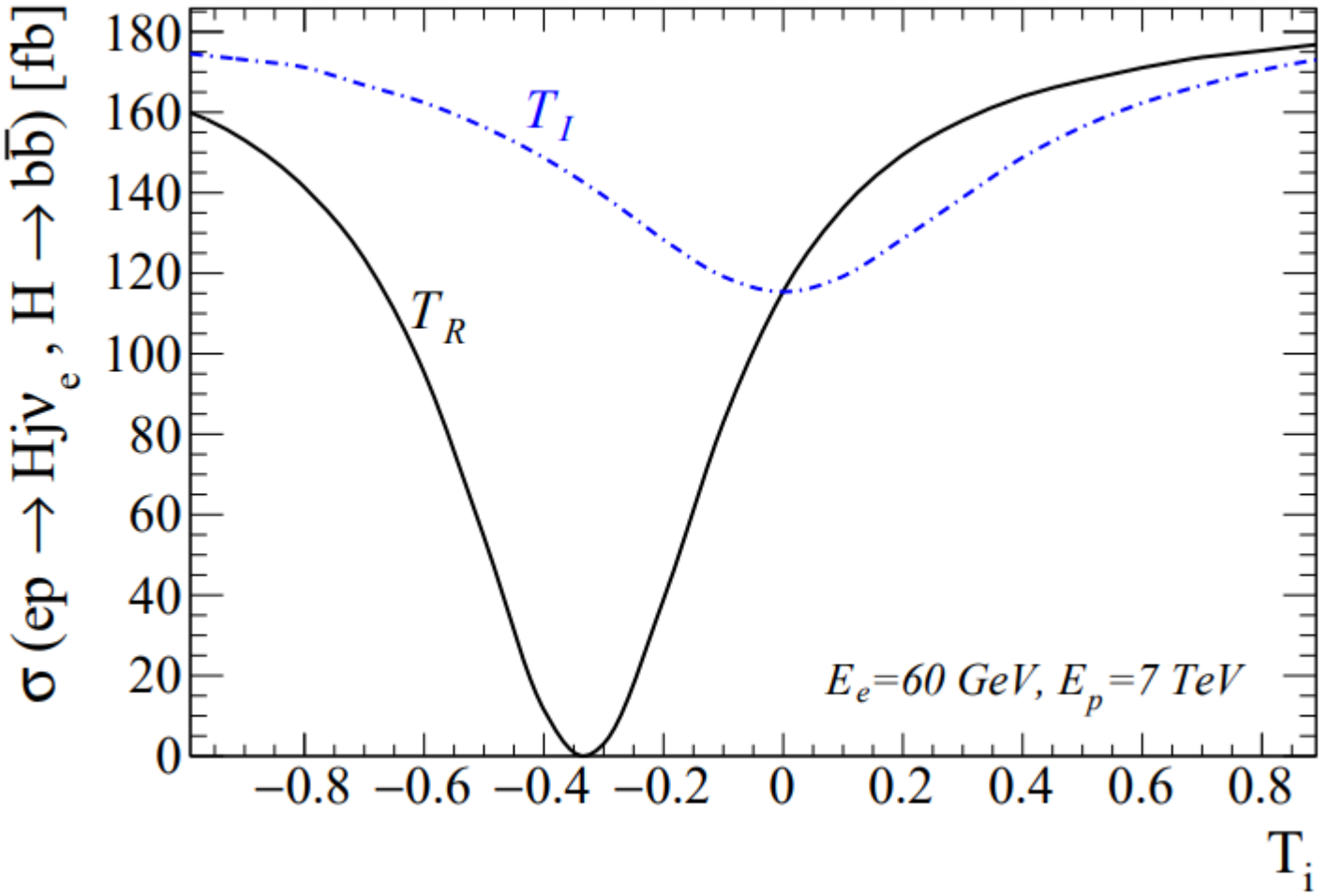

DATA SIMULATION

$$\sigma(e^- p \to H j \nu_e,\ H \to b\bar{b})(T_i) = \sigma_{\mathrm{SM}} + \alpha_i T_i + \beta_i T_i^2,$$

- Signal cross section as a function of T_I and T_R coefficients
- For $T_R = -1/3$ cross section goes to zero.
- SM cross section is shown at $T_i = 0$

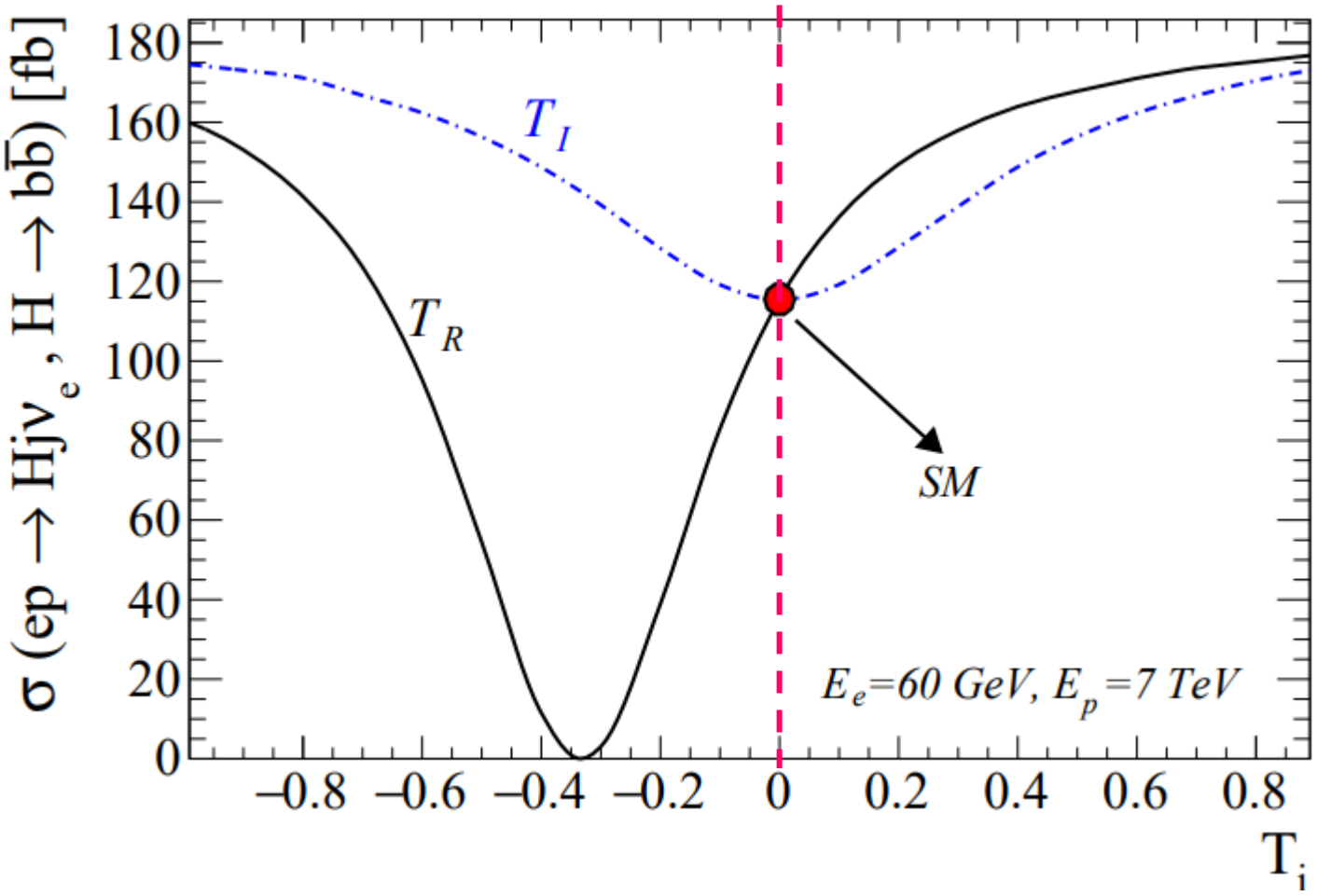

DATA SIMULATION

$$\sigma(e^- p \to H j \nu_e,\ H \to b\bar{b})(T_i) = \sigma_{\mathrm{SM}} + \alpha_i T_i + \beta_i T_i^2,$$

- Signal cross section as a function of T_I and T_R coefficients
- For $T_R = -1/3$ cross section goes to zero.
- SM cross section is shown at $T_i = 0$
- **Negative values are appeared.**

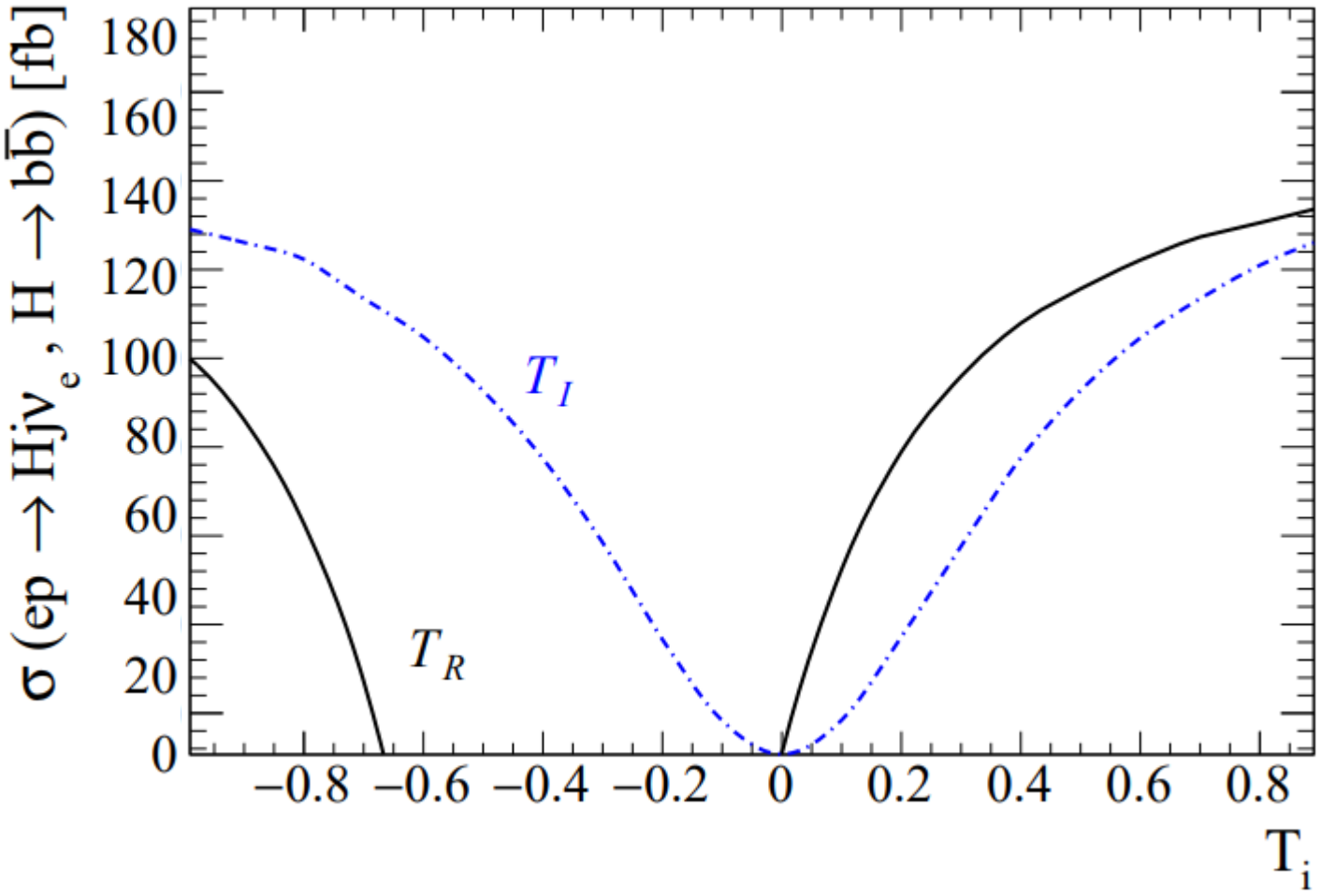

DATA SIMULATION

$$\sigma(e^- p \to H j \nu_e,\ H \to b\bar{b})(T_i) = \sigma_{\mathrm{SM}} + \alpha_i T_i + \beta_i T_i^2,$$

- Signal cross section as a function of T_I and T_R coefficients
- For $T_R = -1/3$ cross section goes to zero.
- SM cross section is shown at $T_i = 0$
- Negative values are appeared.
- Two areas will be probed for T_R

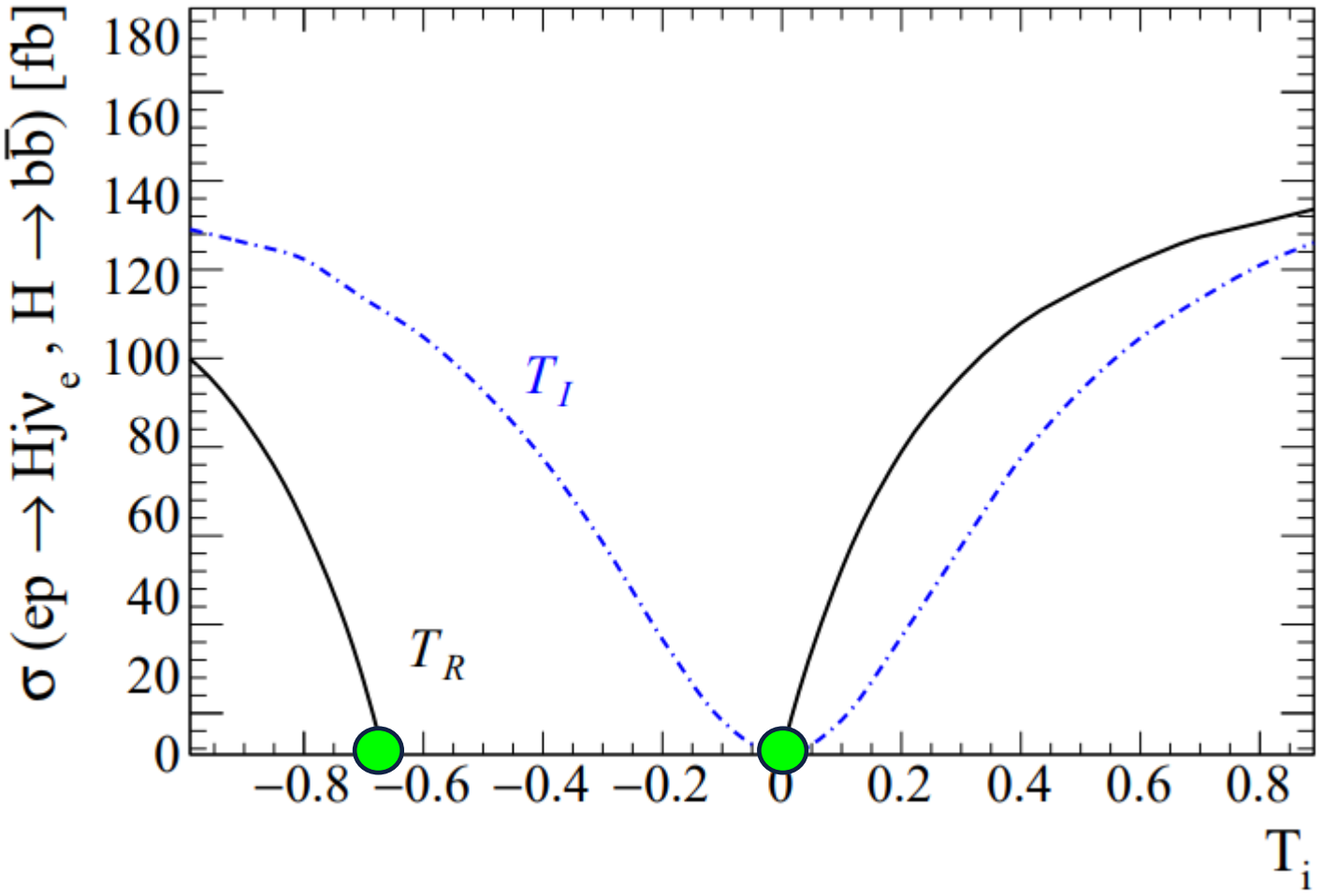

DATA SIMULATION

- LHeC & FCC-eh benchmarks

C.M. Energy (TeV)	1.3	3.46	3.46	3.46
Integrated luminosity (ab^{-1})	1.0	1.0	2.0	10.0

Signal process

$e^- p \to H j \nu_e$, where $H \to b\bar{b}$

L_{eff}

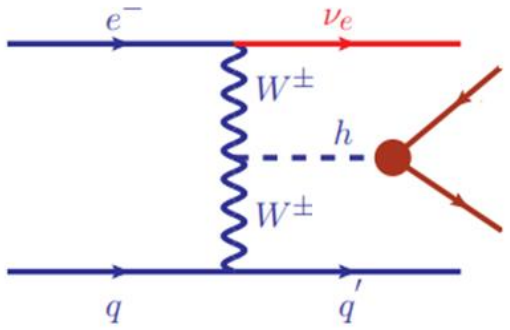

Background processes

- $e^- p \to H j \nu_e$, $H \to b\bar{b}$ (SM irreducible background),
- $e^- p \to Z j \nu_e$, $Z \to b\bar{b}$,
- $e^- p \to Z j \nu_e$, $Z \to c\bar{c}$,
- $e^- p \to V^* j \nu_e$, $V^* \to b\bar{b}$ $(V = \gamma, g)$,
- $e^- p \to V^* j \nu_e$, $V^* \to c\bar{c}$ $(V = \gamma, g)$,
- $e^- p \to V^* j \nu_e$, $V^* \to j_\ell \bar{j}_\ell$ $(V = Z, \gamma, g,\ j_\ell = u, d, s)$,
- $e^- p \to \bar{t} j \nu_e$, $\bar{t} \to W^- \bar{b}$, $W^- \to jj$.

DATA SIMULATION

- **Backgrounds Feynman diagrams**

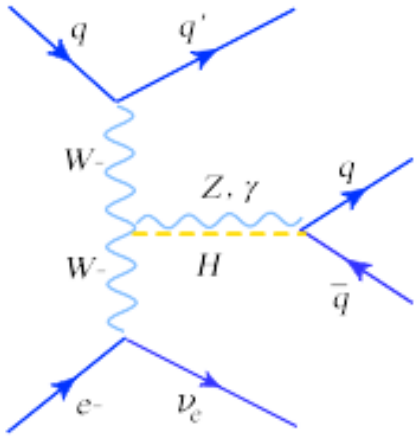

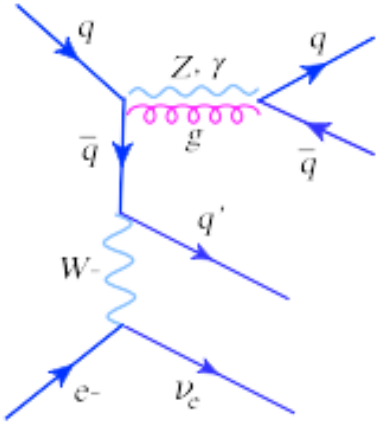

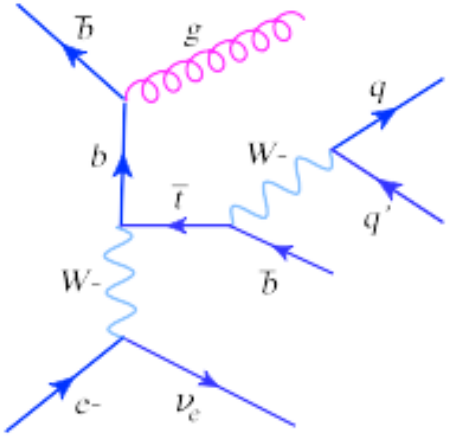

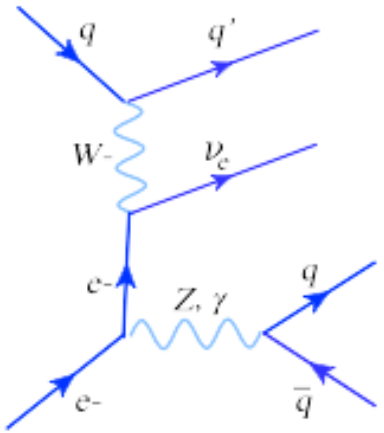

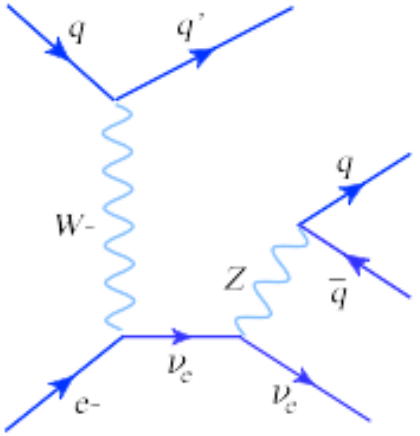

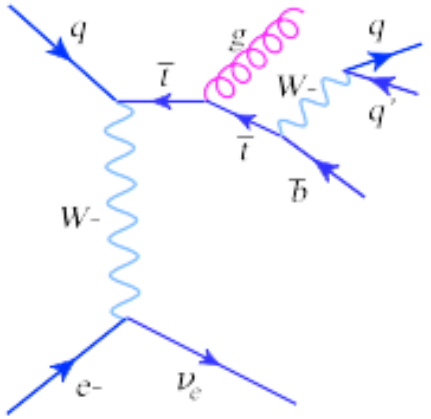

ANALYSIS STRATEGY

Event selection (pre-selection cuts)

- Exactly 2 b-tagged jet
- And 3 jets (Including 1 forward jet)

- $P_T > 20$ GeV for all jets
- $|\eta| \leq 2.5$ for b-tagged jets
- $\Delta R > 0.5$ GeV for all objects
- $|\eta| \leq 5$ for forward jet

- MET > 20 GeV
- Isolated lepton veto

$I_{rel} < 0.1$ $I_{rel} = \Sigma p_T^i / p_T^{\mathrm{P}}$

ANALYSIS STRATEGY

Event selection (pre-selection cuts)

- Exactly 2 b-tagged jet
- And 3 jets (Including 1 forward jet)

- $P_T > 30$ GeV for all jets
- $|\eta| \leq 2.5$ for b-tagged jets
- $\Delta R > 0.5$ GeV for all objects
- $|\eta| \leq 5$ for forward jet ($-1 < \eta < 5$)

- MET > 20 GeV
- Isolated lepton veto

$I_{rel} < 0.1$ $I_{rel} = \Sigma p_T^i / p_T^{\mathrm{P}}$

η of the forward jet in ep collision

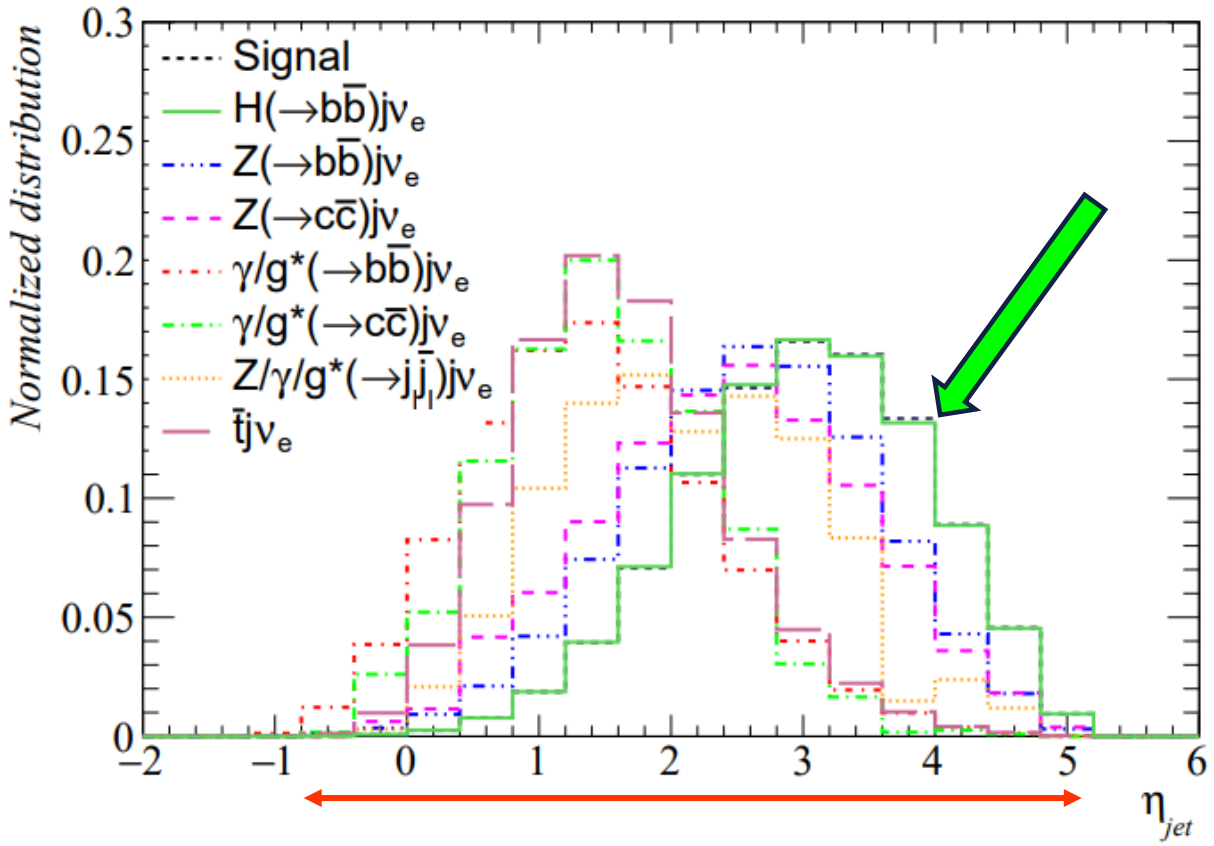

ANALYSIS STRATEGY

- **Event selection efficiencies for T_R=0 and for SM backgrounds**

$\sqrt{s}$ [TeV]	$T_R = 0.1$	$H(\to b\bar{b})j\nu_e$	$Z(\to b\bar{b})j\nu_e$	$Z(\to c\bar{c})j\nu_e$
1.3	0.145	0.145	0.111	6.9×10^{-4}
3.46	0.090	0.090	0.065	3.1×10^{-4}
$\sqrt{s}$ [TeV]	$\gamma/g^*(\to b\bar{b})j\nu_e$	$\gamma/g^*(\to c\bar{c})j\nu_e$	$Z/\gamma/g^*(\to j\ell\bar{j}\bar{\ell})j\nu_e$	$\bar{t}j\nu_e$
1.3	0.015	4.9×10^{-4}	4.8×10^{-5}	0.052
3.46	9.2×10^{-3}	2.3×10^{-4}	4.7×10^{-5}	0.025

ANALYSIS STRATEGY

- **Event selection efficiencies for T_R=0 and for SM backgrounds**

$\sqrt{s}$ [TeV]	$T_R = 0.1$	$H(\to b\bar{b})j\nu_e$	$Z(\to b\bar{b})j\nu_e$	$Z(\to c\bar{c})j\nu_e$
1.3	0.145	0.145	0.111	6.9×10^{-4}
3.46	0.090	0.090	0.065	3.1×10^{-4}
$\sqrt{s}$ [TeV]	$\gamma/g^*(\to b\bar{b})j\nu_e$	$\gamma/g^*(\to c\bar{c})j\nu_e$	$Z/\gamma/g^*(\to j\ell\bar{j}\bar{\ell})j\nu_e$	$\bar{t}j\nu_e$
1.3	0.015	4.9×10^{-4}	4.8×10^{-5}	0.052
3.46	9.2×10^{-3}	2.3×10^{-4}	4.7×10^{-5}	0.025

To enhance the sensitivity, we perform a multivariate analysis (MVA)

ANALYSIS STRATEGY

Input variables

According to Ranking input variables

- $M_{b_1 b_2}$: invariant mass of the two b-tagged jets,
- $\alpha_{b_1 b_2}^{\mathrm{COM}}$: angle between the momentum vectors of the b-tagged jets as measured in the center-of-momentum (COM) frame of the b-jets,
- η_{jet}: pseudorapidity of the non-b-tagged jet,
- $\Delta R_{b_1 b_2}$: distance between the two b-tagged jets,
- $\Delta R_{b_1 j}$: distance between the leading b-tagged jet and the non-b-tagged jet,
- $\Delta R_{b_2 j}$: distance between the sub-leading b-tagged jet and the non-b-tagged jet,
- $\cos \alpha_{b_1 b_2}$: cosine of the angle between the momentum vectors of two b-tagged jets,
- $\not{E}_T$: missing transverse energy,
- H_T: scalar sum of transverse momenta of all objects reconstructed in the detector.

ANALYSIS STRATEGY

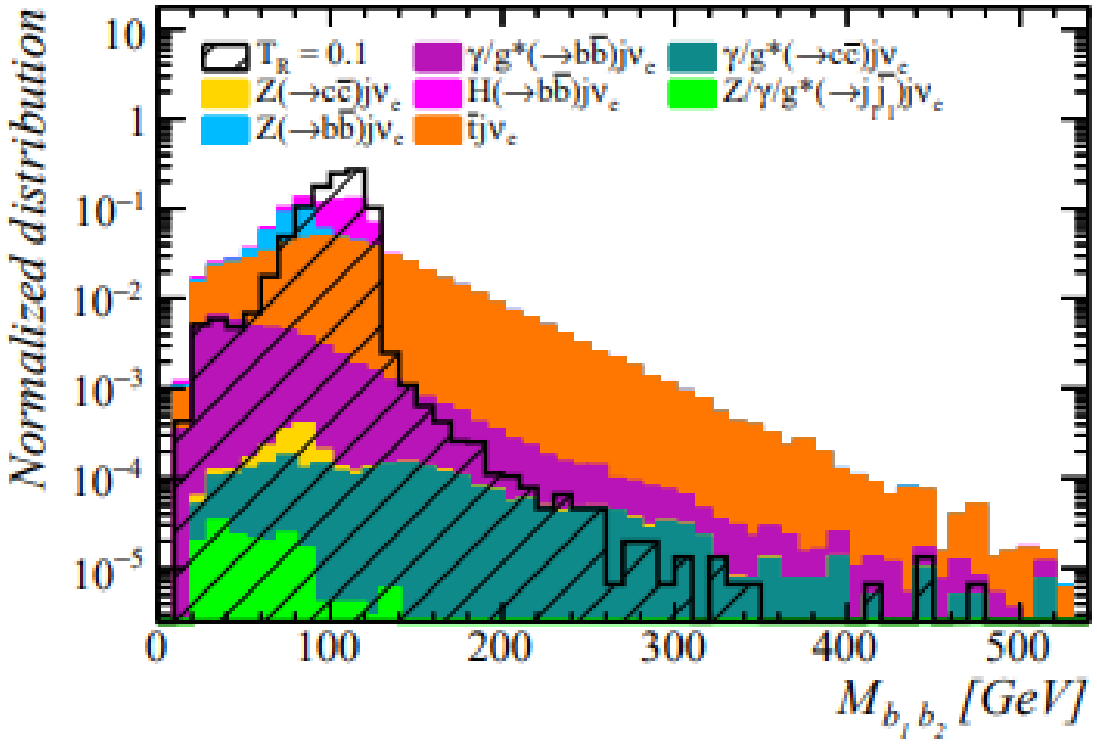

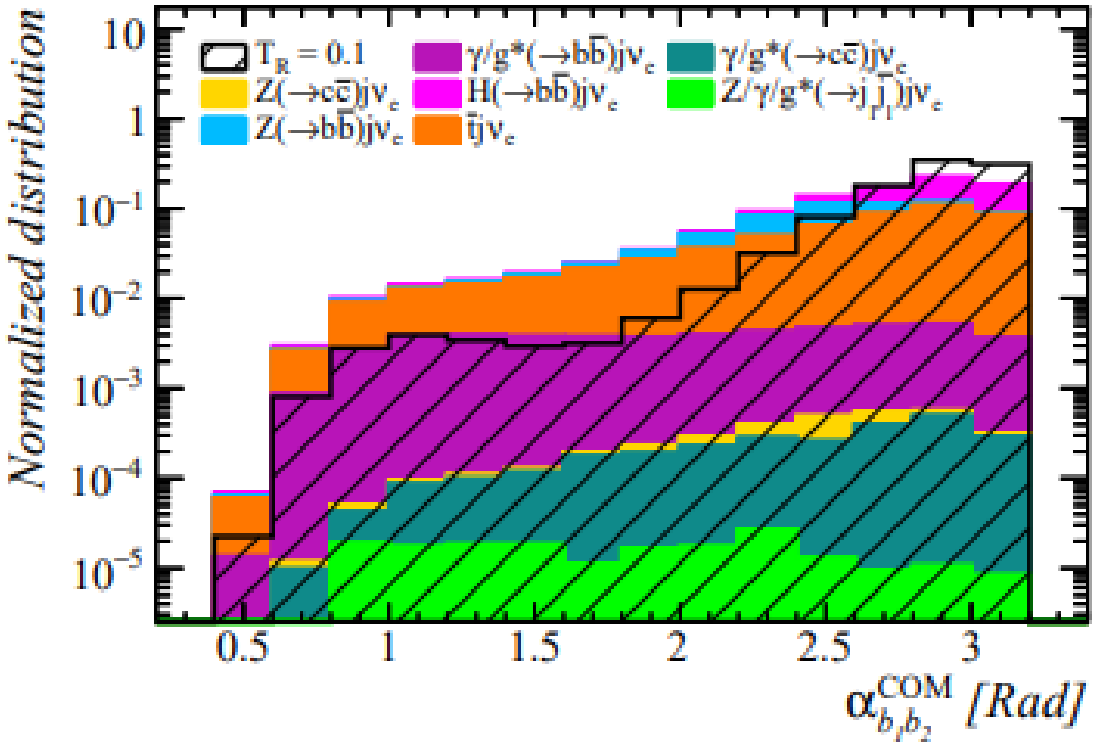

ANALYSIS STRATEGY

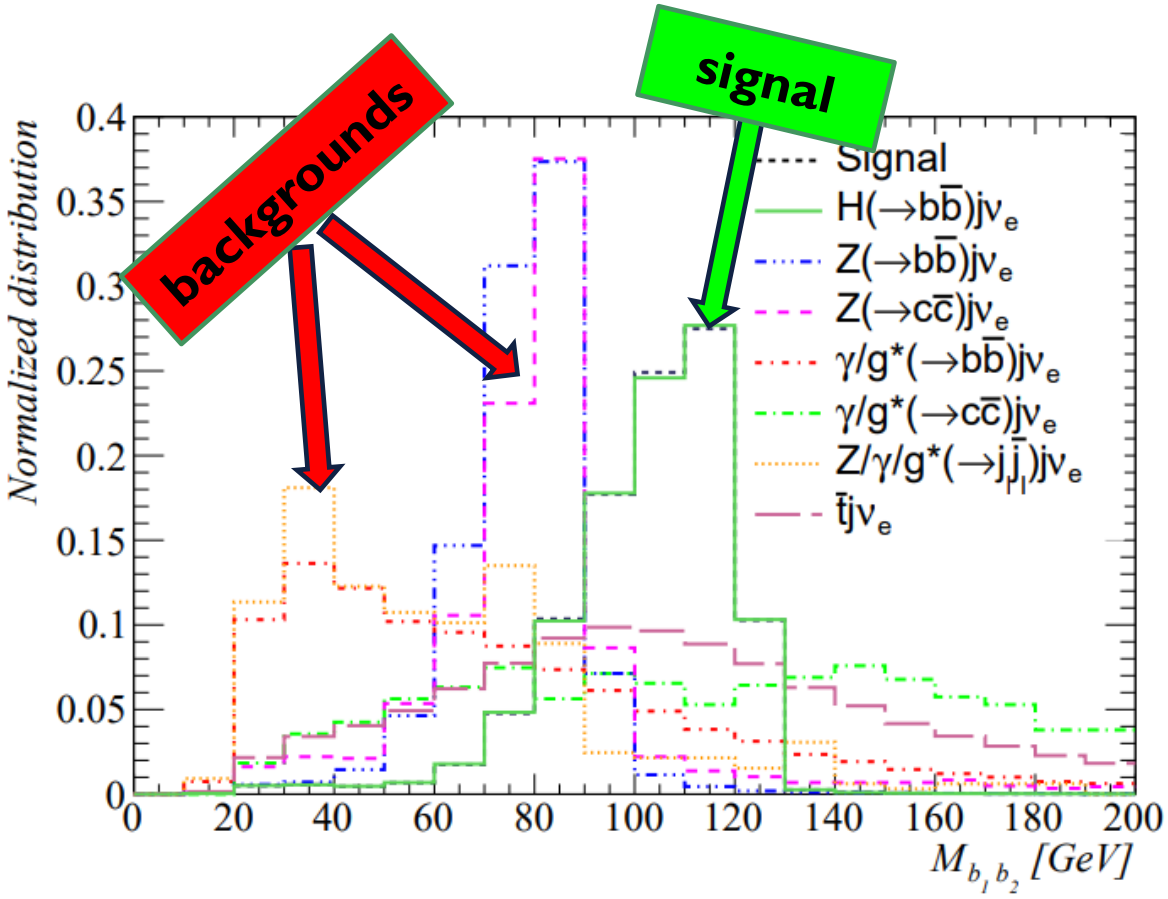

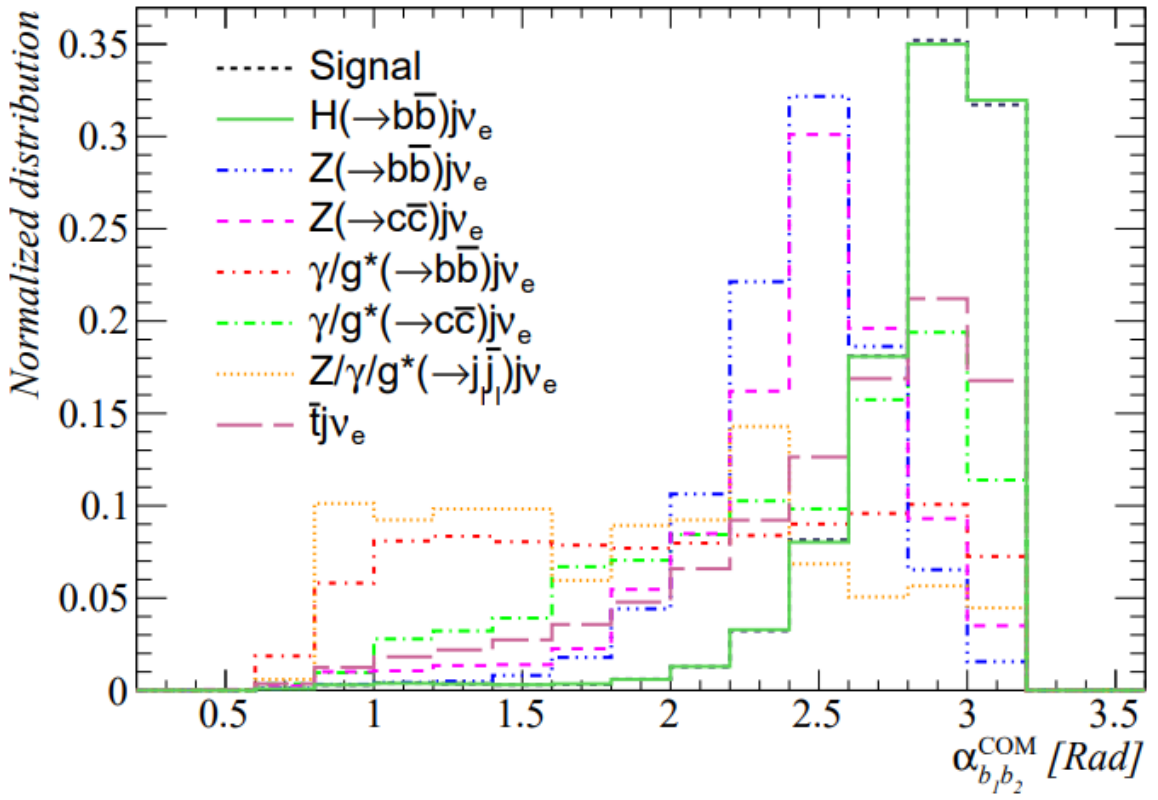

ANALYSIS STRATEGY

- **Correlation Matrix**

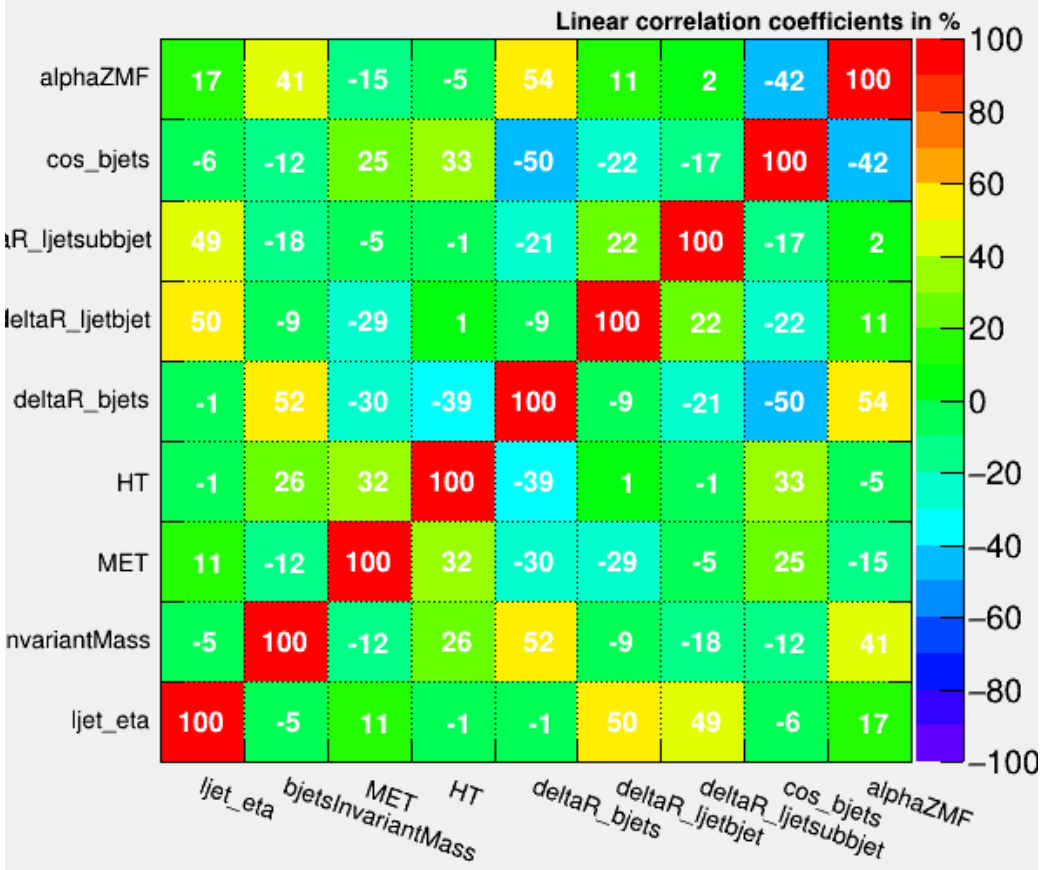

- **ROC curve**

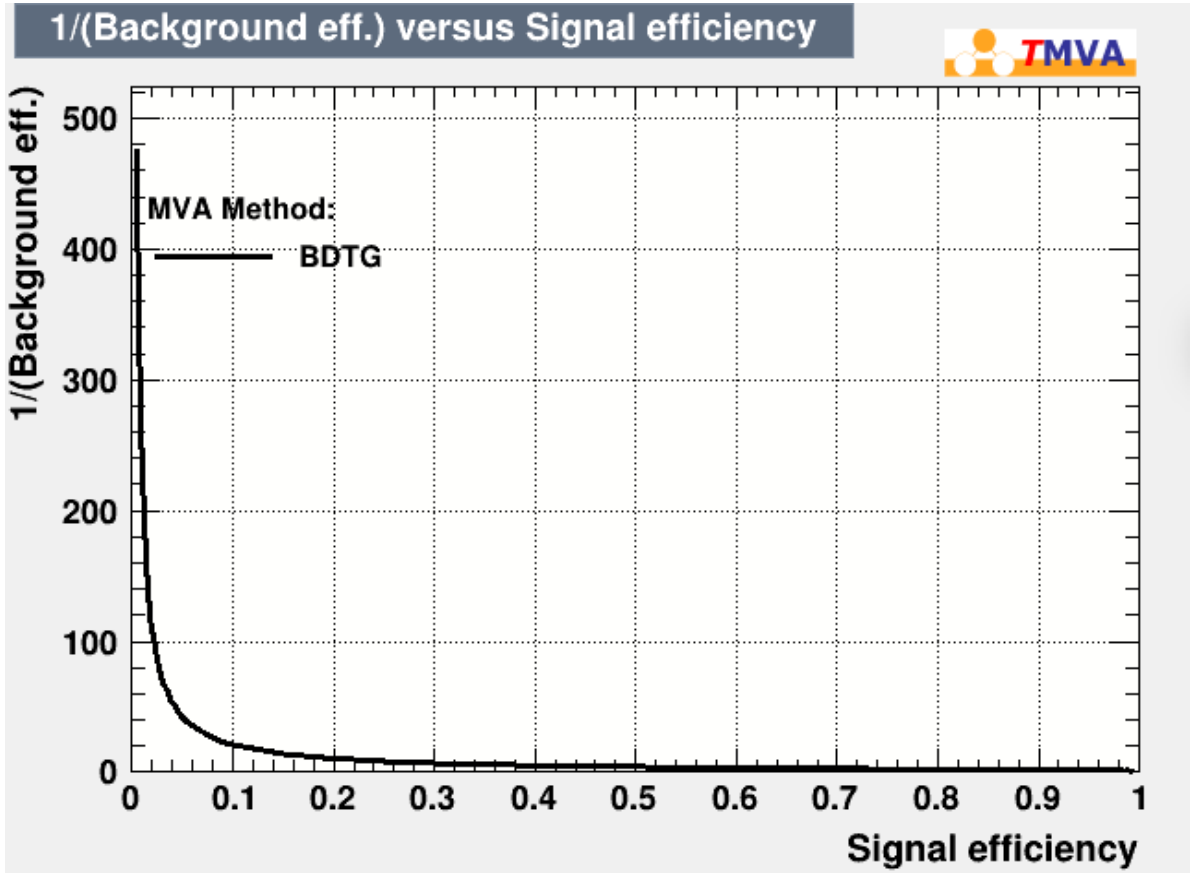

ANALYSIS STRATEGY

- **Gradient Boosted Decision Tree Method**

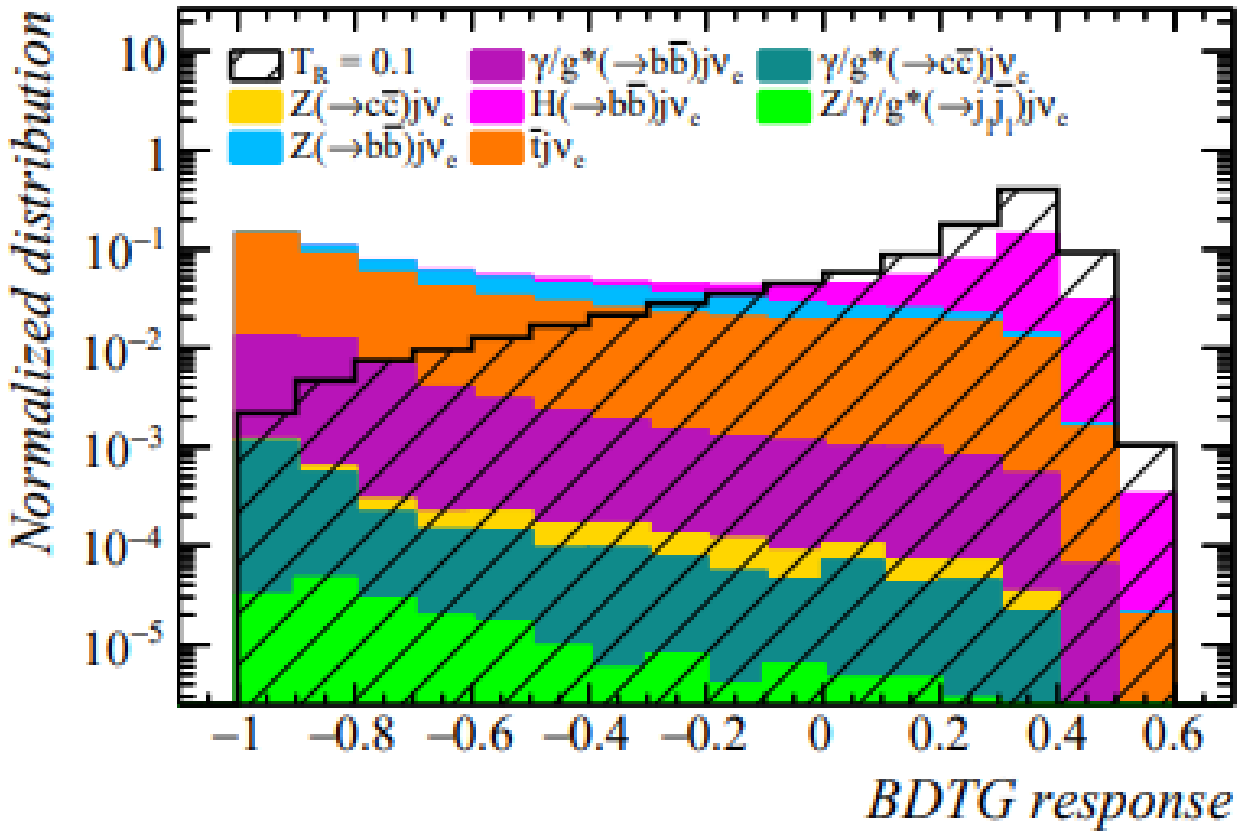

RESULTS

$\sqrt{s}$ [TeV]	$\mathcal{L}$ [ab^{-1}]	T_R	T_I
1.3	1	$[-0.6697, -0.6629] \cup [-0.0037, 0.0031]$ $([-0.6702, -0.6624] \cup [-0.0043, 0.0036])$	$[-0.0460, 0.0460]$ $([-0.0499, 0.0499])$
	2	$[-0.6687, -0.6639] \cup [-0.0027, 0.0021]$ $([-0.6691, -0.6635] \cup [-0.0031, 0.0025])$	$[-0.0381, 0.0381]$ $([-0.0414, 0.0414])$
	10	$[-0.6674, -0.6653] \cup [-0.0014, 0.0008]$ $([-0.6676, -0.6651] \cup [-0.0016, 0.0009])$	$[-0.0238, 0.0238]$ $([-0.0261, 0.0261])$
3.46	1	$[-0.6690, -0.6639] \cup [-0.0026, 0.0025]$ $([-0.6695, -0.6635] \cup [-0.0030, 0.0029])$	$[-0.0409, 0.0409]$ $([-0.0442, 0.0442])$
	2	$[-0.6683, -0.6647] \cup [-0.0019, 0.0017]$ $([-0.6686, -0.6644] \cup [-0.0022, 0.0020])$	$[-0.0342, 0.0342]$ $([-0.0370, 0.0370])$
	10	$[-0.6673, -0.6657] \cup [-0.0009, 0.0007]$ $([-0.6674, -0.6655] \cup [-0.0010, 0.0009])$	$[-0.0224, 0.0224]$ $([-0.0243, 0.0243])$

	T_R	T_I
$\mu_{b\bar{b}}$	$[-0.55, -0.46] \cup [-0.12, 0.33]$	$[-0.43, 0.43]$
d_e	–	$[-0.09, 0.09]$

arXiv:2003.00099

RESULTS

$\sqrt{s}$ [TeV]	$\mathcal{L}$ [ab^{-1}]	T_R	T_I
1.3	1	$[-0.6697, -0.6629] \cup [-0.0037, 0.0031]$ $([-0.6702, -0.6624] \cup [-0.0043, 0.0036])$	$[-0.0460, 0.0460]$ $([-0.0499, 0.0499])$
	2	$[-0.6687, -0.6639] \cup [-0.0027, 0.0021]$ $([-0.6691, -0.6635] \cup [-0.0031, 0.0025])$	$[-0.0381, 0.0381]$ $([-0.0414, 0.0414])$
	10	$[-0.6674, -0.6653] \cup [-0.0014, 0.0008]$ $([-0.6676, -0.6651] \cup [-0.0016, 0.0009])$	$[-0.0238, 0.0238]$ $([-0.0261, 0.0261])$
3.46	1	$[-0.6690, -0.6639] \cup [-0.0026, 0.0025]$ $([-0.6695, -0.6635] \cup [-0.0030, 0.0029])$	$[-0.0409, 0.0409]$ $([-0.0442, 0.0442])$
	2	$[-0.6683, -0.6647] \cup [-0.0019, 0.0017]$ $([-0.6686, -0.6644] \cup [-0.0022, 0.0020])$	$[-0.0342, 0.0342]$ $([-0.0370, 0.0370])$
	10	$[-0.6673, -0.6657] \cup [-0.0009, 0.0007]$ $([-0.6674, -0.6655] \cup [-0.0010, 0.0009])$	$[-0.0224, 0.0224]$ $([-0.0243, 0.0243])$

	T_R	T_I
$\mu_{b\bar{b}}$	$[-0.55, -0.46] \cup [-0.12, 0.33]$	$[-0.43, 0.43]$
d_e	–	$[-0.09, 0.09]$

arXiv:2003.00099

RESULTS

- **The coefficients marginalized bounds at 95% CL:**

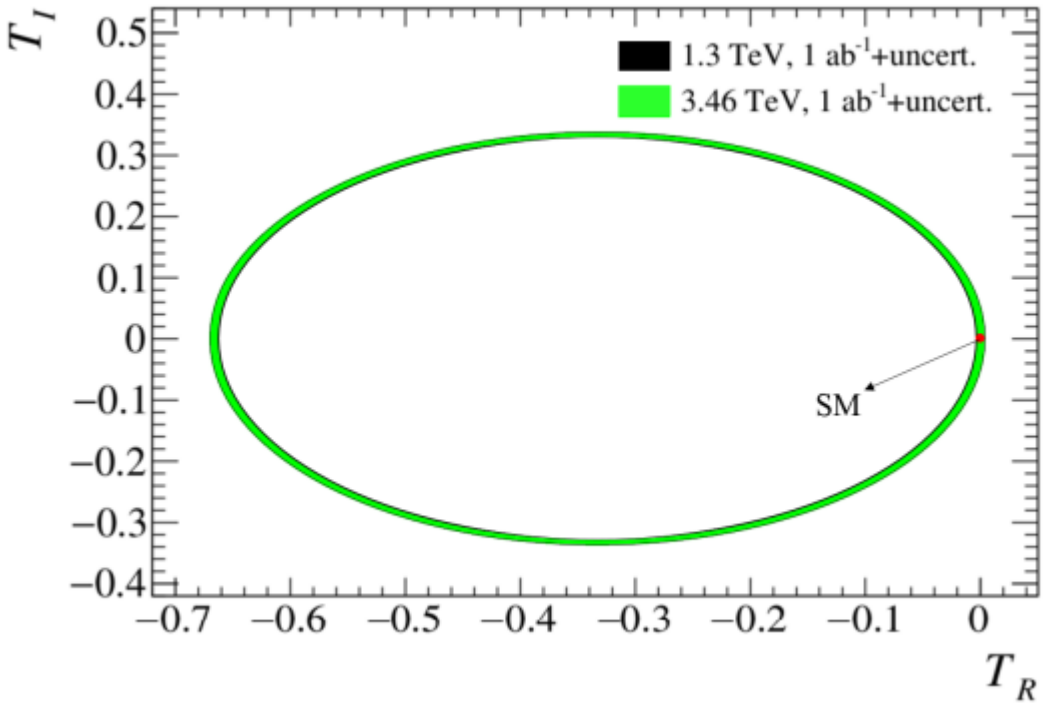

arXiv:2003.00099

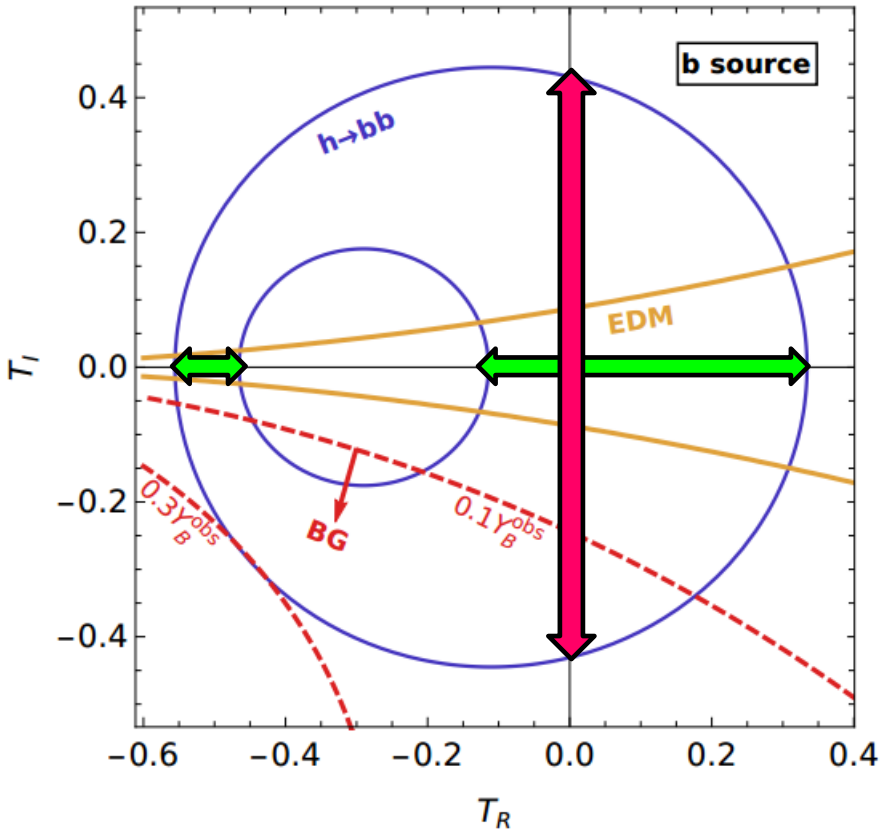

RESULTS

- **The coefficients marginalized bounds at 95% CL:**

arXiv:2003.00099

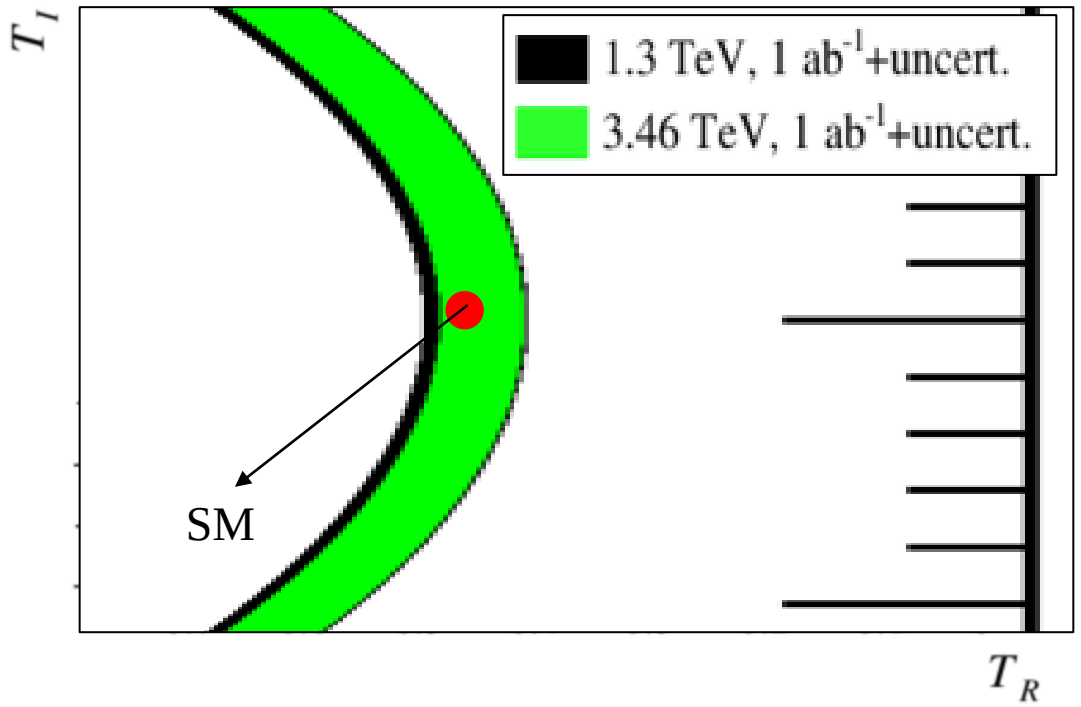

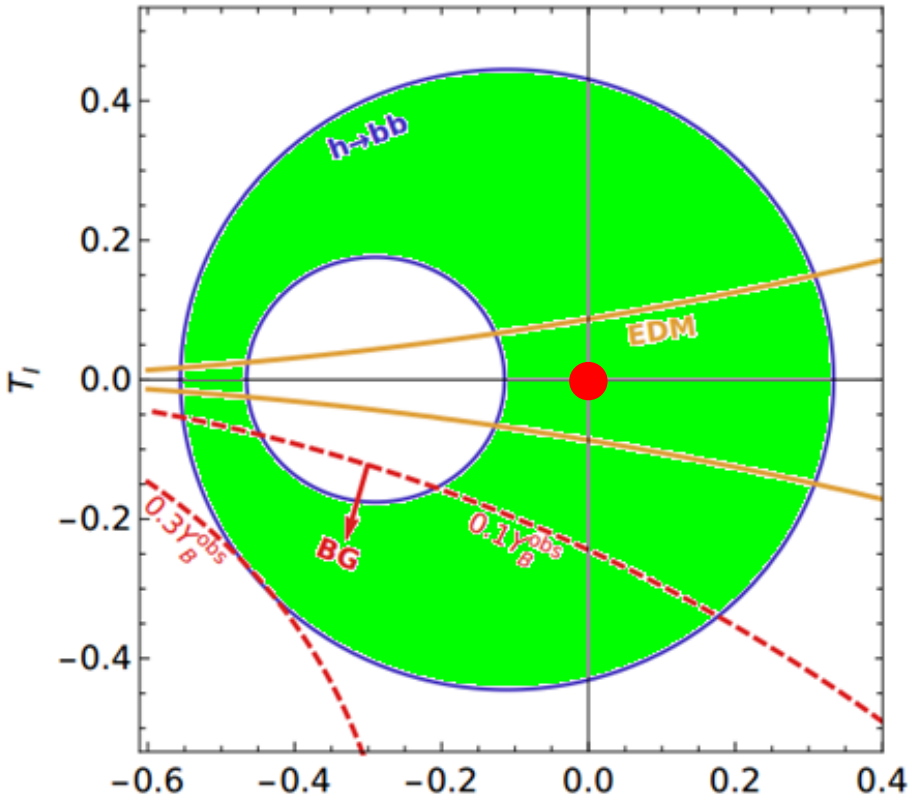

RESULTS

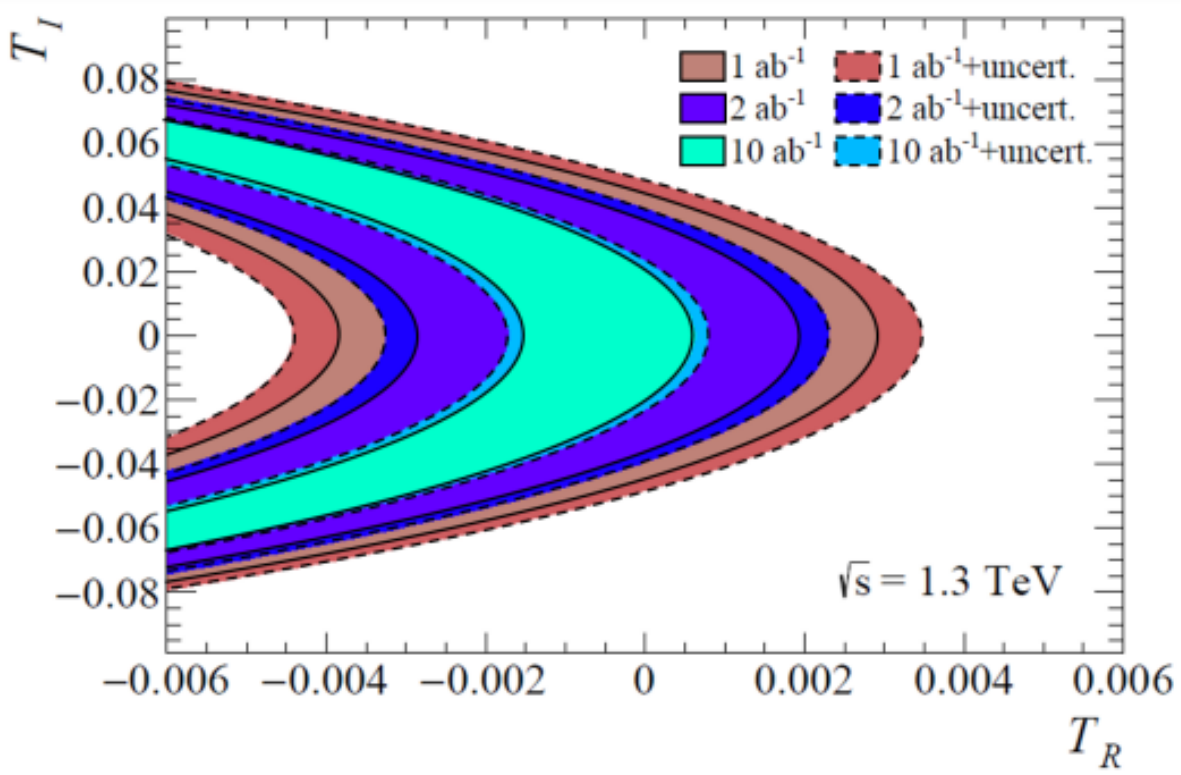
T_I
0.08
0.06
0.04
0.02
0
−0.02
−0.04
−0.06
−0.08
1 ab^{-1}
1 ab^{-1}+uncert.
2 ab^{-1}
2 ab^{-1}+uncert.
10 ab^{-1}
10 ab^{-1}+uncert.
$\sqrt{s}$ = 1.3 TeV
−0.006 −0.004 −0.002 0 0.002 0.004 0.006
T_R

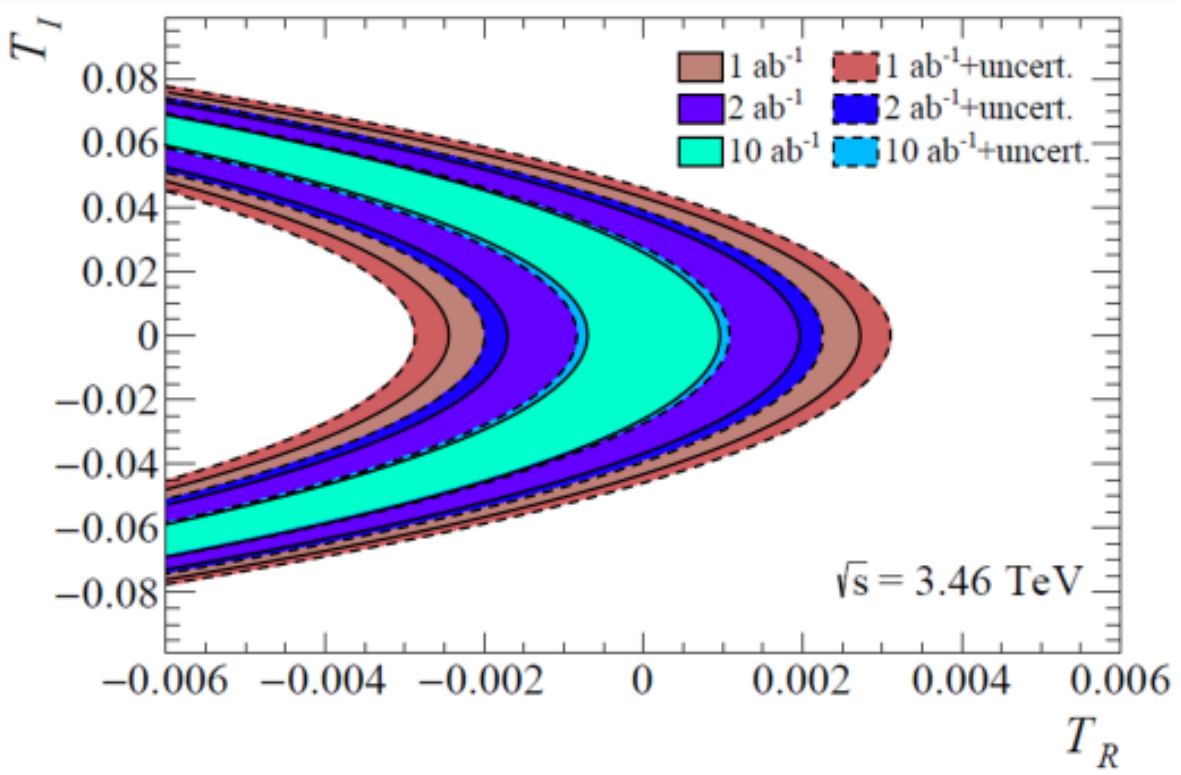
T_I
0.08
0.06
0.04
0.02
0
−0.02
−0.04
−0.06
−0.08
1 ab^{-1}
1 ab^{-1}+uncert.
2 ab^{-1}
2 ab^{-1}+uncert.
10 ab^{-1}
10 ab^{-1}+uncert.
$\sqrt{s}$ = 3.46 TeV
−0.006 −0.004 −0.002 0 0.002 0.004 0.006
T_R

RESULTS

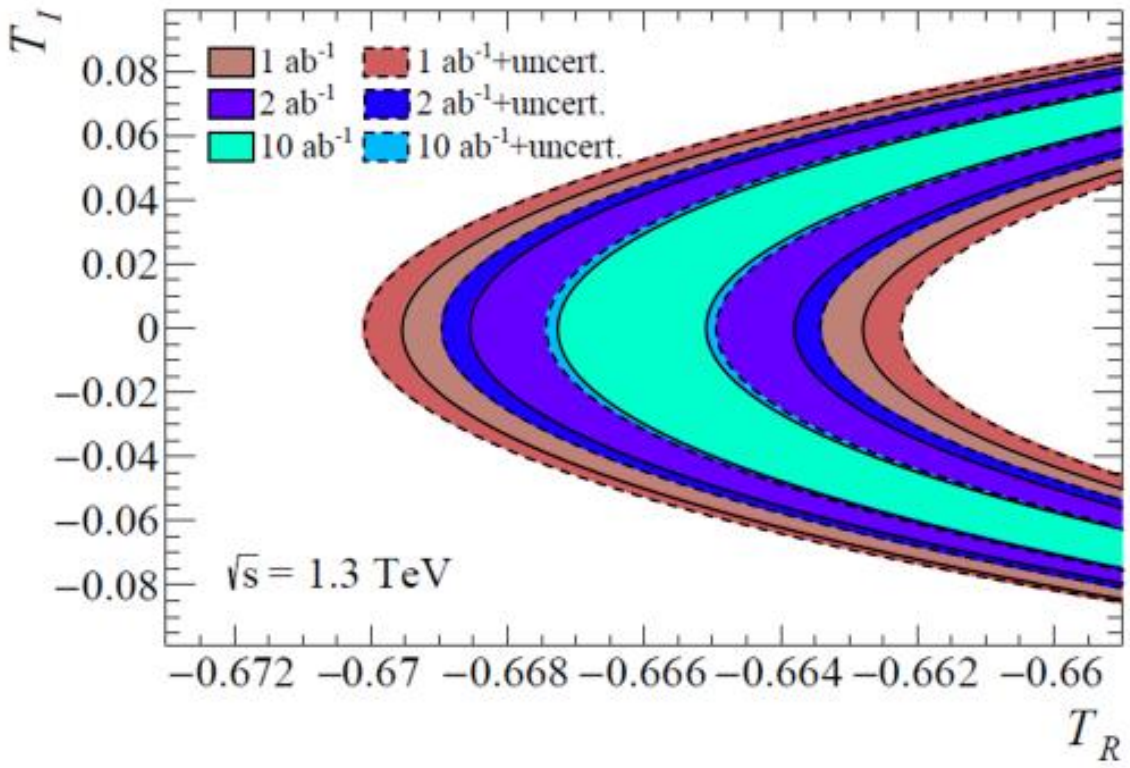
T_I
0.08
0.06
0.04
0.02
0
−0.02
−0.04
−0.06
−0.08
1 ab^{-1}
2 ab^{-1}
10 ab^{-1}
1 ab^{-1}+uncert.
2 ab^{-1}+uncert.
10 ab^{-1}+uncert.
$\sqrt{s}$ = 1.3 TeV
−0.672 −0.67 −0.668 −0.666 −0.664 −0.662 −0.66
T_R

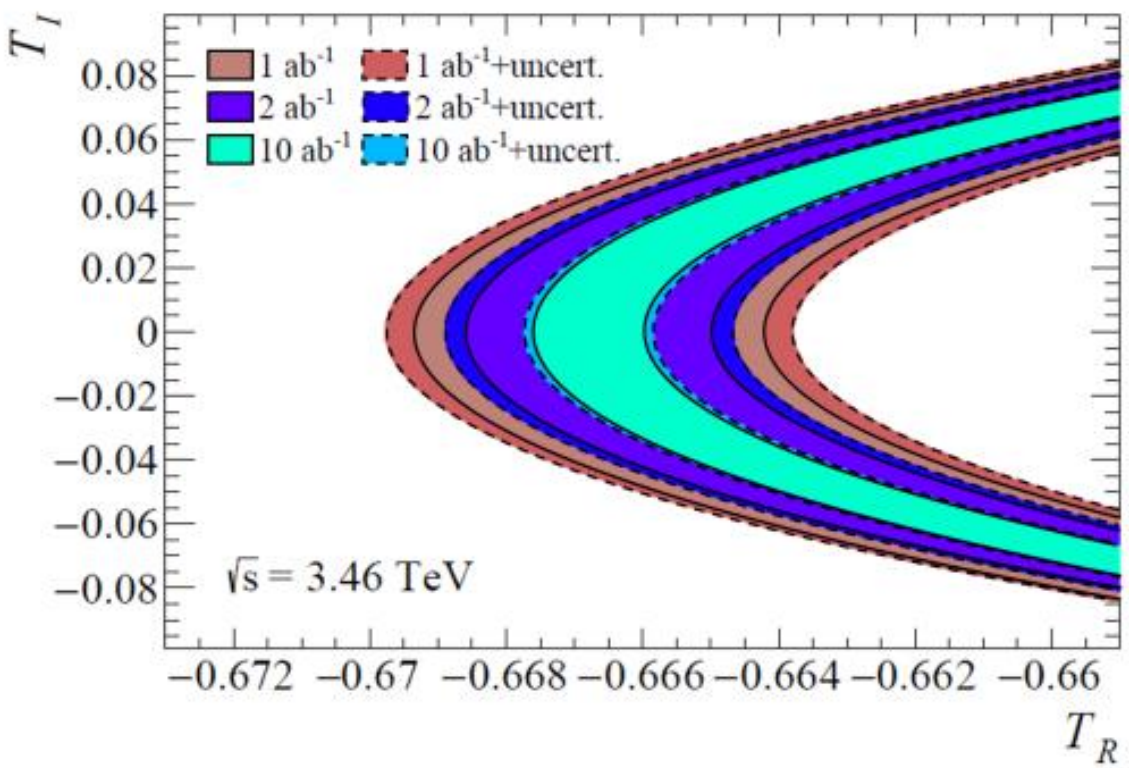
T_I
0.08
0.06
0.04
0.02
0
−0.02
−0.04
−0.06
−0.08
1 ab^{-1}
2 ab^{-1}
10 ab^{-1}
1 ab^{-1}+uncert.
2 ab^{-1}+uncert.
10 ab^{-1}+uncert.
$\sqrt{s}$ = 3.46 TeV
−0.672 −0.67 −0.668 −0.666 −0.664 −0.662 −0.66
T_R

CONCLUSION

- After the Higgs boson discovery, the focus shifted toward understanding its couplings to other particles, in particular to the fermions. CP violation in the Higgs sector impact on Baryogensis
- The Yukawa coupling of h to the 3rd generation fermions is larger.
- A crucial aspect is the measurement of the b-quark Yukawa coupling, and the observation of the $H \rightarrow bb$ decay remains very challenging at the LHC.
- Recently, there has been a consideration for high energy ep collisions with very exiting prospects.
- Effective Lagrangian with dimension-six operators is used to constrain b Yukawa coupling.
- Data simulation for the LHeC and FCC-eh benchmarks.
- A MVA approach with BDTG method is applied to suppress the background contributions.
- Limits at 95% CL on the coupling coefficients have been obtained for two center-of-mass energies of the LHeC and FCC-eh.
- We show that the MVA increases the sensitivity to the b-quark Yukawa couplings.

INSTITUTE FOR RESEARCH IN FUNDAMENTAL SCIENCES

THANKS FOR YOUR ATTENTION!

BACKUP

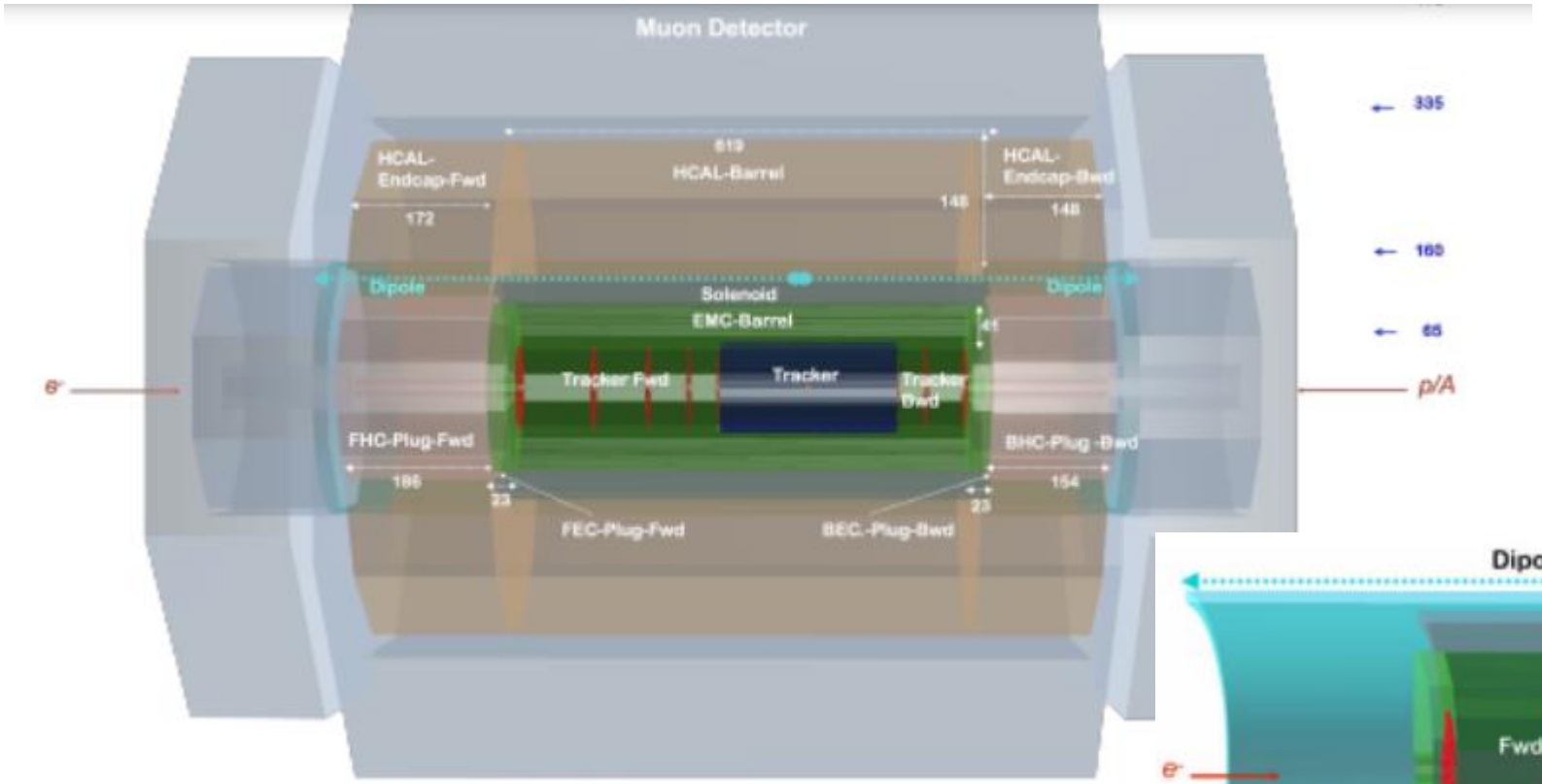
Muon Detector
335
165
65
HCAL-Endcap-Fwd
172
519
HCAL-Barrel
148
HCAL-Endcap-Bwd
148
Dipole
Solenoid
Dipole
EMC-Barrel
Tracker Fwd
Tracker
Tracker Bwd
e⁻
p/A
FHC-Plug-Fwd
186
23
FEC-Plug-Fwd
BEC-Plug-Bwd
23
BHC-Plug -Bwd
154

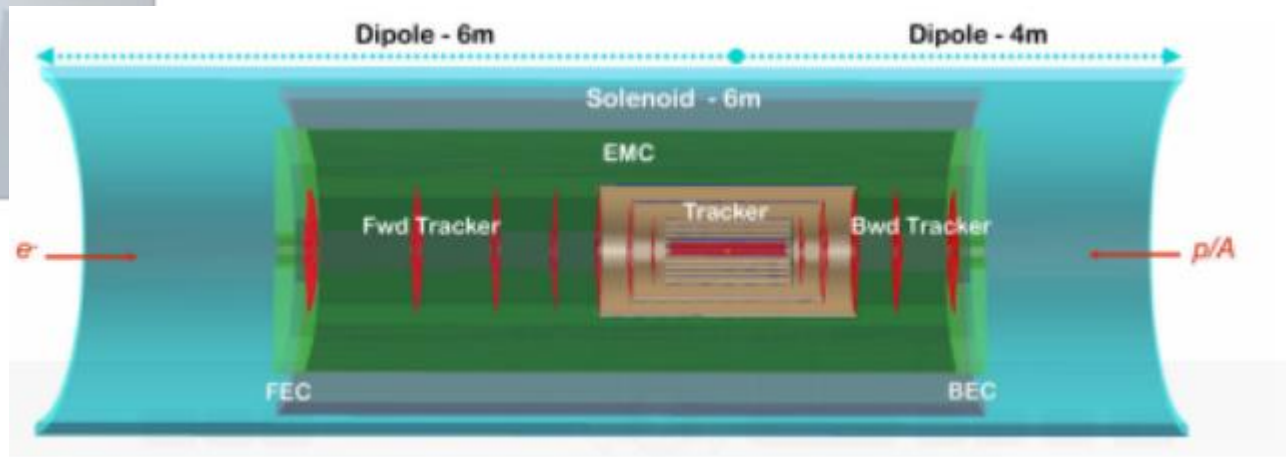
Dipole - 6m
Dipole - 4m
Solenoid - 6m
EMC
Fwd Tracker
Tracker
Bwd Tracker
e⁻
p/A
FEC
BEC